EVALUATION OF CONE BEAM COMPUTED TOMOGRAPHY SIALOGRAPHY IN DIAGNOSING SALIVARY GLAND LESIONS

DISSERTATION

Submitted to The Tamil Nadu Dr. M.G.R Medical University

in partial fulfillment of the requirement for the degree of

MASTER OF DENTAL SURGERY

BRANCH IX

ORAL MEDICINE AND RADIOLOGY

2017 - 2020

CERTIFICATE I

This is to certify that the dissertation titled **"Evaluation of Cone Beam Computed Tomography Sialography in Diagnosing Salivary Gland Lesions"** is a bonafide record of the work done by **Dr. Godwi Femine C.P.,** under our guidance during her postgraduate study period of 2017-2020. The dissertation is submitted to **The Tamil Nadu Dr. M.G.R Medical University, Chennai,** in partial fulfillment of the requirement for the Degree of Master of Dental Surgery in Oral Medicine and Radiology, Branch IX. It has not been submitted (partial or full) for the award of any other degree or diploma.

Guide

Dr. SHASHI KIRAN M., MDS
Associate Professor
Department of Oral Medicine and Radiology
Sree Mookambika Institute of Dental Sciences, Kulasekharam.

Co-Guide

Dr. TATU JOY E., MDS
Professor and HOD
Department of Oral Medicine and Radiology
Sree Mookambika Institute of Dental Sciences, Kulasekharam.

URKUND

Urkund Analysis Result

Analysed Document:	THESIS SOFT - plagerism.docx (D60854980)
Submitted:	12/12/2019 7:51:00 AM
Submitted By:	c.p.godwifemine@gmail.com
Significance:	5 %

Sources included in the report:

Dr.Yazhini_OMR_LD.docx (D55509367)
https://www.researchgate.net/figure/Diagnostic-Discrimination-for-MR-Sialography-and-Digital-Subtraction-Sialography-for_tbl1_11086716
8a96b500-d829-43ee-849a-4e26354a89cc
https://www.researchgate.net/publication/236076836_Assessment_of_the_role_of_cone_beam_computed_sialography_in_diagnosing_salivary_gland_lesions
https://www.ncbi.nlm.nih.gov/pmc/articles/PMC3604366/
https://www.ijirr.com/sites/default/files/issues-pdf/2231.pdf
https://www.researchgate.net/publication/322249933_CBCT_sialography
https://www.researchgate.net/publication/20469225_Digital_subtraction_sialography_conventional_sialography_high-resolution_ultrasonography_and_computed_tomography_in_the_diagnosis_of_salivary_gland_diseases
https://fdocuments.in/document/assessment-of-the-role-of-cone-beam-computed-sialography-in-diagnosing-salivary.html

Instances where selected sources appear:

21

CERTIFICATE II

This is to certify that this dissertation work titled **"Evaluation of Cone Beam Computed Tomography Sialography in Diagnosing Salivary Gland Lesions"** of the candidate **Dr. Godwi Femine C.P.,** with registration Number **241727251** for the award of **MASTER OF DENTAL SURGERY** in the branch of Oral Medicine and Radiology, Branch IX. I personally verified the urkund.com website for the purpose of plagiarism Check. I found that the uploaded thesis file contains from introduction to conclusion pages and result shows **5%** of plagiarism in the dissertation.

Guide & Supervisor sign with Seal.

Date:

Place:

SREE MOOKAMBIKA INSTITUTE OF DENTAL SCIENCES, KULASEKHARAM

ENDORSEMENT BY THE PRINCIPAL / HEAD OF THE INSTITUTION

This is to certify that the dissertation entitled **"Evaluation of Cone Beam Computed Tomography Sialography in Diagnosing Salivary Gland Lesions"** is a bonafide research work done by **Dr. Godwi Femine C.P.,** under the guidance of **Dr. Shashi Kiran., MDS,** Associate Professor, Department of Oral Medicine and Radiology, Sree Mookambika Institute of Dental Sciences, Kulasekharam.

Dr. Elizabeth Koshi, MDS,
PRINCIPAL
Sree Mookambika Institute of Dental Sciences,
V.P.M Hospital Complex,
Padanilam,
Kulasekharam,
Kanyakumari District,
Tamil Nadu - 629161

DECLARATION

I hereby declare that this dissertation **"Evaluation of Cone Beam Computed Tomography Sialography in Diagnosing Salivary Gland Lesions"** is a bonafide record of work undertaken by me and that this thesis or a part of it has not been presented earlier for the award of degree, diploma, fellowship or similar title of recognition.

Dr. Godwi Femine C.P.,
MDS Student
Department of Oral Medicine and Radiology
Sree Mookambika Institute of Dental Sciences
Kulasekharam.

ACKNOWLEDGEMENT

I extend my hearty thanks to my guide ***Dr. Shashi Kiran M., MDS.,*** Associate Professor, Department of Oral Medicine and Radiology for his guidance and constant encouragement in each step of my post graduation programme. I extent my gratitude for his immense patience and full heartedness in all the works, he guided me to perfection. It was a great blessing and opportunity to do my post graduation programme under his valuable guidance.

I am thankful to ***Dr. Tatu Joy. E,*** Professor and HOD, Department of Oral Medicine and Radiology, for his passionate teaching throughout this entire postgraduation programme. I also thank him for his constant enthusiasm and support in all my endeavors. It was a great opportunity to do my postgraduation under him.

I express my gratitude to ***Dr. Elizabeth Koshi,*** Principal, Sree Mookambika Institute of Dental Sciences, Kulasekharam for permitting me to carry out the Dissertation in this Institution.

I would also like to extent my sincere gratitude to my teachers ***Dr. Rahul R,*** Reader, ***Dr. Redwin Dhas Manchil P,*** Reader, ***Dr. Farakath Khan M***, and ***Dr. Lakshmi P.S.,*** Senior Lecturers for their constant encouragement throughout this PG curriculum.

I would like to acknowledge the support given by ***Dr. Velayuthan Nair,*** Chairman and ***Dr. Rema V Nair,*** Director, Sree Mookambika Institute of Medical Sciences, for the academic support to carry out my study in this Institution.

I owe my hearty thanks to my batch mates ***Dr. Maria Monisha A*** and ***Dr. Janetha Edwin*** for standing together with me in all my ups and downs. I feel happy to do my PG curriculum along with them. I thank my seniors, ***Dr. Tanuja S, Dr. Dhanya S.V.*** and ***Dr. Sajitha Jamin S.L***. for their support in this post-graduation programme.

I would like to also extend my hearty gratitude to my fellow postgraduates ***Dr. Reshmi M, Dr. Leema R.K., Dr. Abijah R.S., Dr Anusha J.A., Dr. Ashifa Bebe M.M.*** and ***Dr. Vivek S*** for all the emotional support they gave me throughout this PG curriculum.

I owe my sincere love and acknowledgement to my father and role model, ***Mr. Chellan T.K.,*** for always standing beside me and to my mother, ***Mrs. Pushpa Latha D*** for being my first guru, whose principles I follow till date. I would also like to extend my love to my sister, ***Ms. Didwi Femine C.P.*** for her constant enthusiasm.

Last, but not the least I thank God Almighty for his profound blessings, wisdom, health and strength he has showered over me.

CONTENTS

LIST OF ABBREVIATIONS

CBCT	Cone Beam Computed Tomography
CT	Computed Tomography
USG	Ultrasonography
MRI	Magnetic Resonance Imaging
PET	Positron Emission Tomography
TPT	Technetium-99m pertechnetate
FDG	2-[18] fluoro- 2-deoxy D-glucose

LIST OF FIGURES

LIST OF TABLES

LIST OF GRAPHS

LIST OF COLOR PLATES

Color Plate No.	Title of Color Plate
CP-1	Sialography Kit
CP-2	Multiformatted view of CBCT Sialography images

LIST OF ANNEXURES

Annexure No	Contents
1	RESEARCH COMMITTEE CERTIFICATE
2	ETHICAL COMMITTEE CERTIFICATE
3	DATA ENTRY SHEET

ABSTRACT

ABSTRACT

Aim & Objectives:

The aim of this study was to assess the efficacy of cone-beam computed tomography (CBCT) sialography imaging in the evaluation of normal ductal anatomy along with various salivary gland pathosis.

Materials and Methods:

This study comprised of 15 archival CBCT images of patients with signs and symptoms of salivary gland pathologies. A proposed algorithm for evaluation was used to assess and interpret the CBCT images. Four blinded experts manipulated and evaluated the images and scores were given for the interpretation of the images according to the proposed algorithm. Analysis of the resulting data was performed to evaluate the concordance among interpretations. Finally the results were tabulated in "Microsoft Excel" and was evaluated according to consensus and statistical analysis based on "Chi square test".

Results:

The results proved to have inter-observer concordance between the radiologists in interpreting the normal ductal anatomy and various salivary gland pathologies. Assessment of normal ductal anatomy such as primary duct, secondary duct and parenchyma showed no significant inter-observer variability. Abnormal salivary glands findings such as the presence of sialolith, strictures, acinar pooling and space occupying lesions showed similar results between the observers except that of ductal dilatation, which proved to have inter-observer variability between the

radiologists. Hence by, CBCT sialography proved to have superior diagnostic value in revealing the ductal architecture and in the detection of salivary gland pathosis.

Conclusion:

The diagnostic value of CBCT sialography in obstructive salivary gland diseases with demonstration of the ductal architecture of the gland along with the assessment of salivary gland abnormalities was superior. It is a novel technique for imaging major salivary glands by combining the benefits of the sialography with the versatility of the CBCT.

Keywords: Cone-Beam Computed Tomography, Salivary Glands, Sialography

INTRODUCTION

INTRODUCTION

Major salivary glands are most commonly affected by obstructive or inflammatory conditions affecting nearly 1% of the population.[1]They may manifest clinically as a lateral swelling on the face or diffuse enlargement of the gland accompanied by certain symptoms like obstruction or inflammation. Diagnosis of these conditions may be challenging. Radiographic examination is essential in diagnosing such conditions, and plays a pivotal role in planning further management.[2] Plain radiography, sialography, sialendoscopy, computed tomography (CT),cone-beam CT (CBCT), ultrasonography (US), magnetic resonance imaging (MRI), and nuclear scintigraphy/positron emission tomography (PET) are the various diagnostic techniques used for the detection of salivary gland pathologies.[3] Limited information is obtained by evaluation of the salivary glands by conventional methods because only two-dimensional data of three dimensional structures can be achieved. Three-dimensional (3D) depictions of gland ductal anatomy have only been possible by combining sialography with CT or MRI. In the ever expanding arena of knowledge and information, it is vital for any clinician to remain in touch with latest innovations in the field of one's expertise and apply the same for the benefit of patient care and be ready and willing to accept new trends, find time to learn and practice the technological and diagnostic or treatment advances in the related field.[4]

Sialography was first performed in 1902.[5] In sialography, a contrast medium is injected into the duct of major salivary glands to evaluate the ductal anatomy and the presence of strictures or calculi by enhancing good contrast resolution.[2]CT is

another radiographic technique which helps to detect several salivary gland abnormalities such as sialolith within the salivary gland or duct, bony erosion caused by malignant lesions, and inflammatory diseases such as abscess, major salivary duct dilatation etc. Enhanced CT helps to evaluate the staging of malignant disease involving the salivary glands.[6,7] MR sialography is a non-invasive, non-irradiating alternative imaging technique of assessing ductal abnormalities without ionizing radiation or ductal cannulation.[8,] But, MR sialography is not widely available, not to mention cost and other pitfalls of magnetic resonance imaging.

More recently, CBCT is being commonly used for head, neck and dento-maxillofacial diagnosis which provides relatively high isotropic resolution of anatomic structures at a low dose of radiation. The first dental CBCT system became commercially available for dentomaxillofacial imaging in the year 2001(New Tom QR DVT 9000; Quantitative radiology, Verona Italy).[9] Approximately a single rotation of about 9-40 seconds in CBCT scanner can collect volume data because of the presence of the cone-shaped x-ray beam and two-dimensional detectors. They offer the visualization of tissues of the maxillofacial region.[10] CBCT sialography, apparently remains the most efficient method in detection of salivary gland pathologies. This modality might prove useful for demonstrating areas of complex anatomy. However, there is lacunae of studies which depicts the efficacy of CBCT in the diagnosis of salivary gland pathology. In this study, further investigation on the potentials of CBCT sialography were to be assessed along with its efficacy in the diagnosis of salivary gland lesions and an attempt will be made to propose a systematic algorithm to evaluate CBCT sialograms.

AIM AND OBJECTIVES

AIMS AND OBJECTIVES

- To determine the effectiveness of CBCT sialography to evaluate the normal ductal anatomy.
- To determine the effectiveness of CBCT sialography to evaluate the abnormal salivary gland findings such as ductal dilatation, strictures, acinar pooling etc.
- To determine the effectiveness of CBCT sialography to evaluate the salivary gland pathologies such as sialolithiasis, space occupying lesions etc.
- To propose a systematic algorithm for the interpretation of CBCT sialograms.

REVIEW OF LITERATURE

REVIEW OF LITERATURE

A. ANATOMY OF SALIVARY GLANDS:

In humans, the three pairs of major salivary glands are the parotid, submandibular and sublingual glands. The anatomical architecture of all these glands are the same with the secretory acinar within the glands, producing the saliva and the ductal structure that opens into the oral cavity, expelling the saliva.[11]

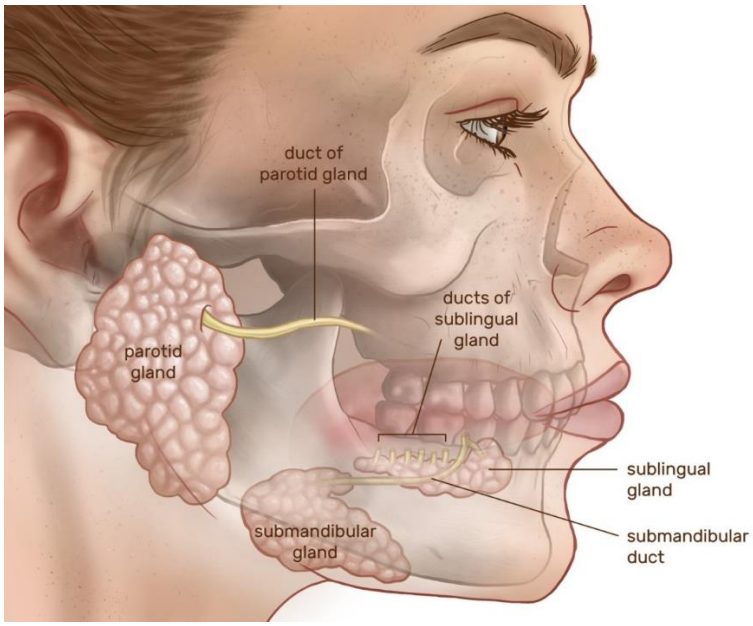

Figure 1: Major salivary glands

Parotid glands are the largest salivary glands which are paired, weighing approximately 14 and 28 gms each.[12,13] The facial nerve (cranial nerve VII) exits the skull through the stylomastoid foramen, pierces the posterior surface of the gland and runs through its parenchyma in anterioinferior direction, lateral to the retromandibular vein.[13] Inside the parenchyma of the gland, the nerve then divides into its five terminal branches (temporal, zygomatic, buccal, mandibular, and cervical).[12-14] The anatomic plan created by the facial nerve divides the parotid

gland into superficial and deep lobes. Glandular tissue located lateral to the plane is considered to be the part of superficial lobe and medial to the plane is considered to be the part of deep lobe.[13] Later, Som et al stated that this landmark is anatomically incorrect, because he believed that the posterior border of the mandibular ramus to be a more accurate dividing line.[13] Using this, the larger superficial lobe of the parotid gland lies lateral to the mandibular ramus, masseter muscles, anterioinferior to the external auditory meatus extending superoinferiorly from the zygomatic arch to the angle of the mandible. In contrast, the smaller deep lobe of the parotid gland lies posterior- medial to the mandibular ramus, anterior to the styloid process and the carotid sheath. Both anatomic landmarks for dividing the parotid lobes are currently in use.[13]

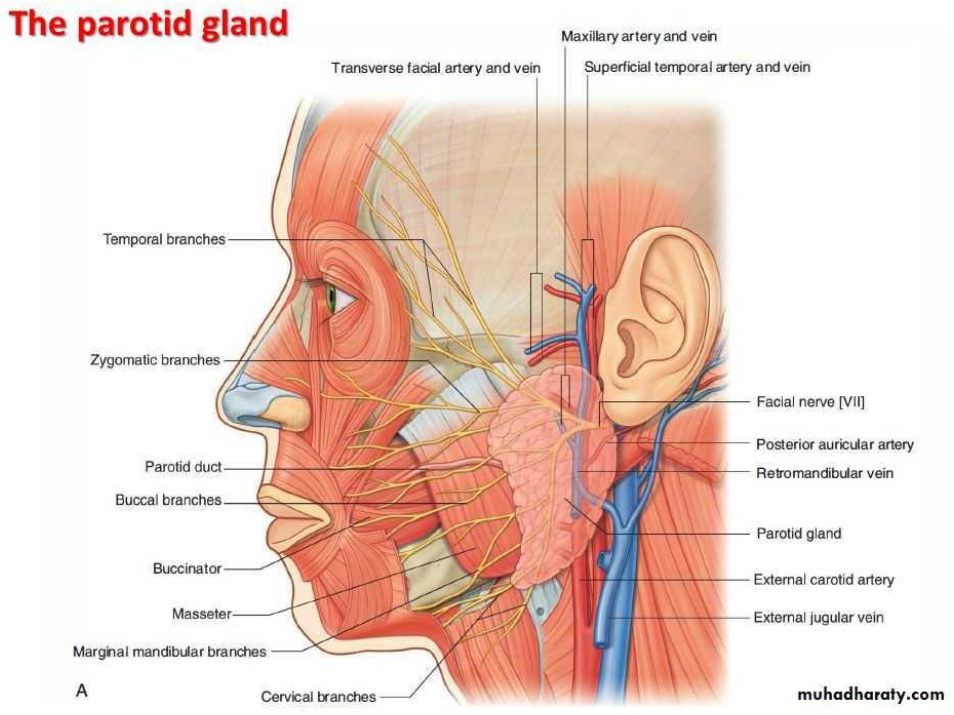

Figure 2: Anatomy of parotid gland

The parotid duct called the Stensen's duct leaves the anterior border of the superficial lobe and runs an anterior course that is inferior to the zygomatic arch and

superficial to the lateral surface of the masseter muscle. At the anterior border of the masseter muscle the duct turns medially, pierces the buccal fat pad and buccinator muscle to open into the oral cavity, opposite to the maxillary second molar.[12,14] Stensen's duct measures approximately 6 cm to 7 cm in length with a lumen caliber of 1 mm to 2 mm. Accessory parotid tissue is present, approximately in 20% of the population and is usually found anterior to the superficial lobe and superior to Stensen's duct.[13]

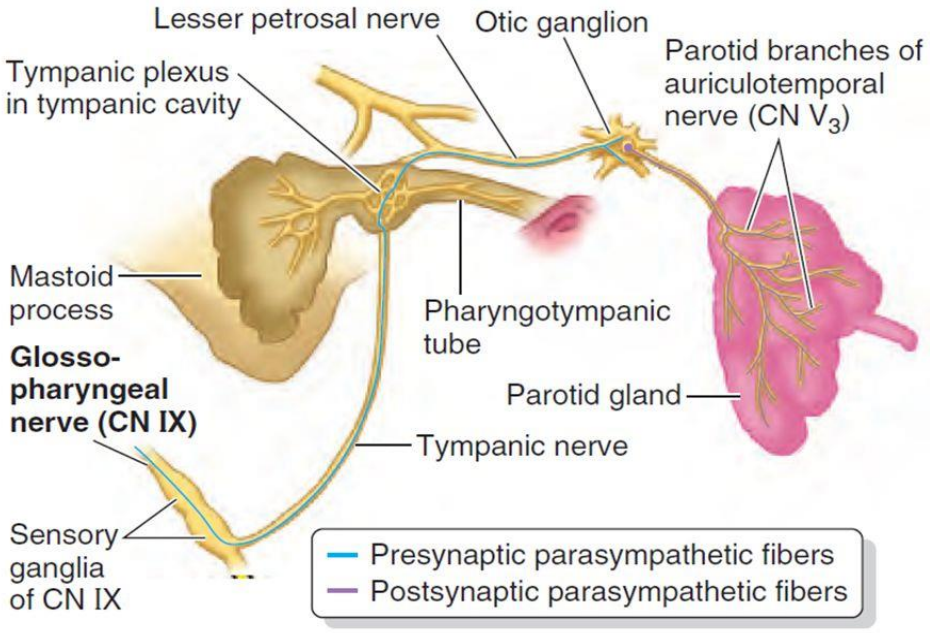

Figure 3: Innervation of parotid gland

Parasympathetic innervation of the parotid gland regulating the secretion, is from the glossopharyngeal nerve (cranial nerve IX) which has a synapses in the otic ganglion and reaches the gland via the auriculotemporal nerve (branch of the mandibular division of the trigeminal nerve, cranial nerve X). [12,14]Sympathetic innervation regulating the vasoconstriction, is derived from the sympathetic plexus of the carotid artery.[13] Blood supply is by branches of the external carotid artery.[13,14]

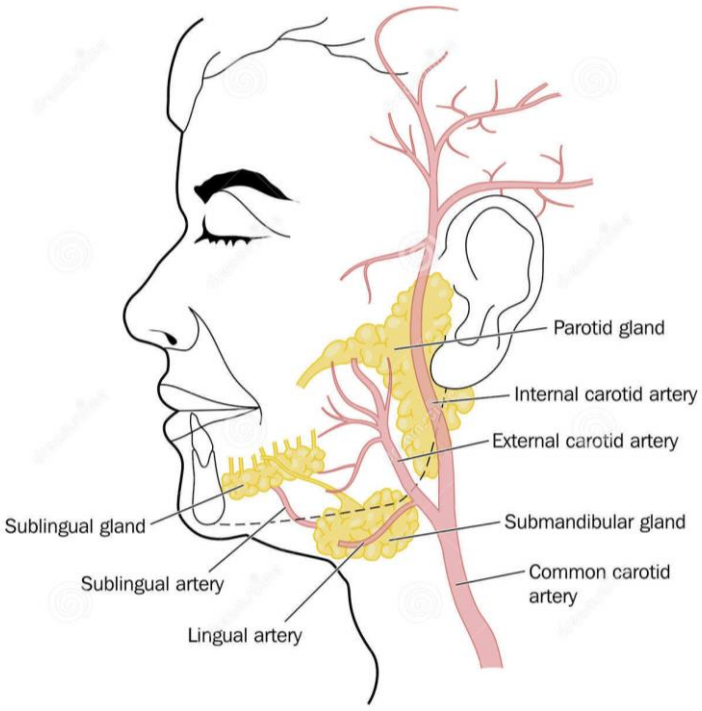

Figure 4: Blood supply of major salivary glands

The submandibular gland is the second largest salivary gland, weighing approximately 10 and 15 grams. It is divided into two lobes by the posterior free border of the mylohyoid muscle.[14] The larger superficial lobe is located in the submandibular triangle between the mylohyoid muscle and the mandibular fossa on the medial aspect of the posterior mandibular body.[13,14] The smaller deep lobe, on the other hand, lies superior to the mylohyoid muscle in the posterior floor of the mouth, medial to the mandibular body.[14] The submandibular duct called the Wharton's duct emerges from the deep lobe and courses anterosuperiorly between the sublingual gland laterally and the genioglossus muscle medially to open immediately lateral to the lingual frenum. [13,14]Wharton's duct is approximately 5 cm long with a lumen caliber that ranges between 1 mm and 3 mm.[13] The gland receives parasympathetic innervation from the chorda tympani branch of the facial nerve (cranial nerve VII) through the lingual nerve and the submandibular ganglion.

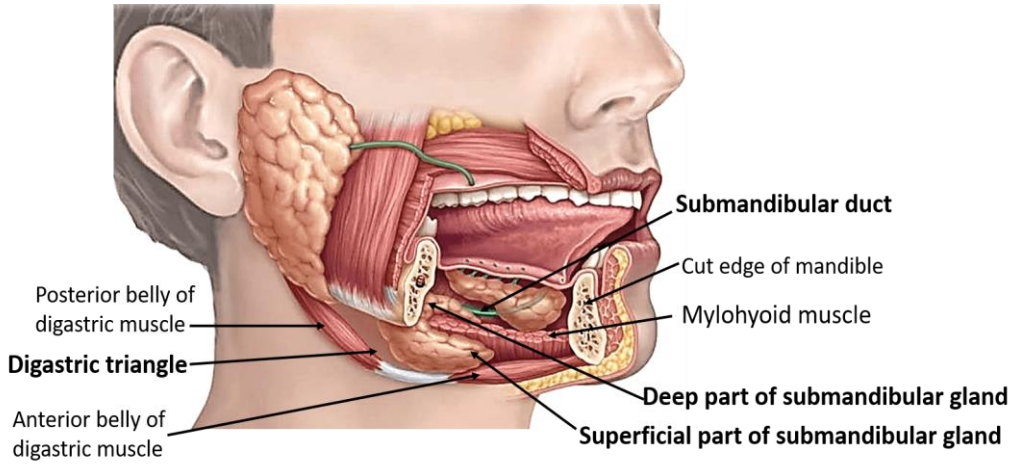

Figure 5: Anatomy of submandibular salivary gland

It receives its sympathetic innervation from the sympathetic plexus around the carotid artery same as parotid gland.[13,14] Blood supply to the submandibular gland is provided by the external maxillary and lingual arteries.[13]

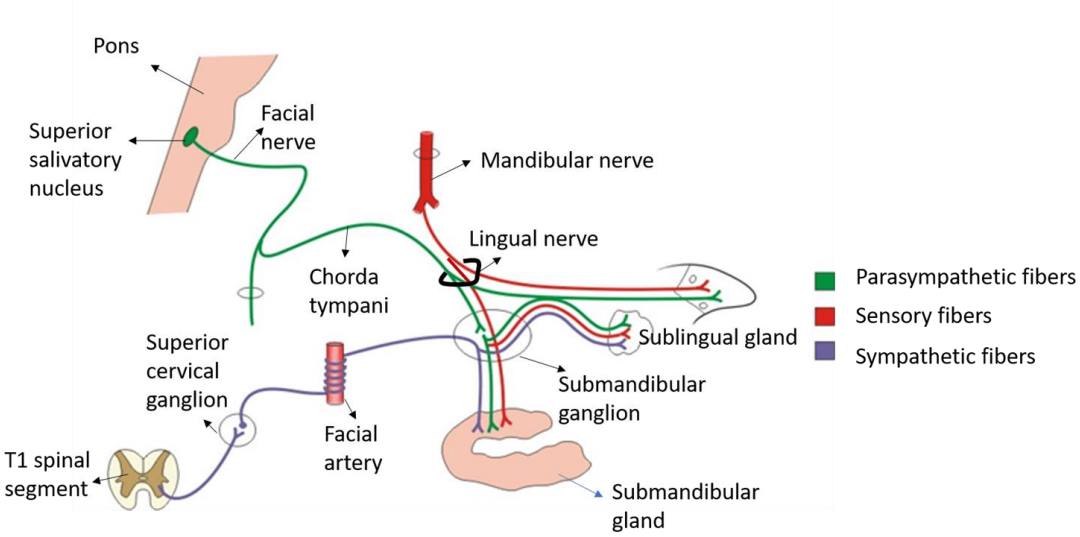

Figure 6: Innervation of submandibular and sublingual salivary gland

The smallest major salivary glands is the sublingual salivary gland weighing approximately 2 to 4 grams, located in the anterior floor of the mouth between the sublingual fossa on the medial aspect of the anterior mandibular body laterally and

the genioglossus muscle medially.[14] It is separated from the genioglossus muscle by the lingual nerve and Wharton's duct.[13] Saliva is secreted into the oral cavity though a number of ducts (the ducts of Rivinus) that open like pores upwards into the sublingual fold.[12-14] Occasionally, these ducts fuse and form Bartholin's duct which opens into Wharton's duct.[13] Nerve supply to the sublingual gland is identical to the submandibular gland but the blood supply is provided by the sublingual artery.[14]

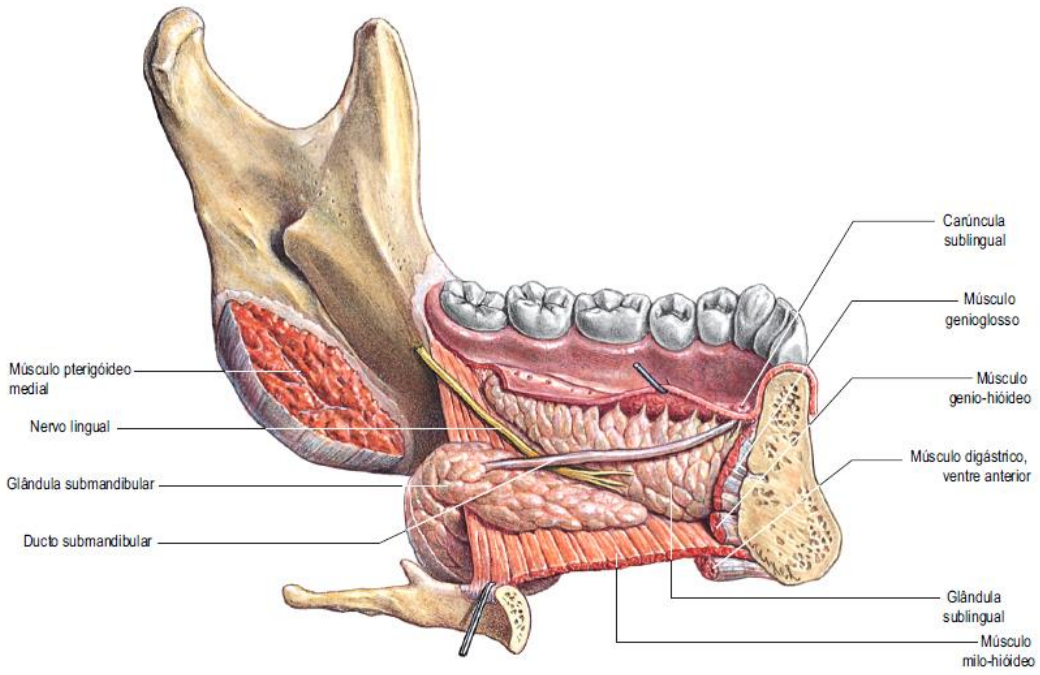

Figure 7: Anatomy of sublingual salivary gland

The minor salivary glands are estimated to be between 600 and 1000 in numbers, scattered throughout the oral submucosa with the exception of the anterior hard palate and gingiva.[12] They are also found in the submucosa of the paranasal sinuses, pharynx, larynx, trachea, and bronchi. Depending on their location, they receive autonomic secretory innervations from several ganglia including the pterygopalatine, otic, and submandibular ganglions.[13]

B. HISTOLOGY OF SALIVARY GLANDS:

The structure of all major salivary glands follows the same general pattern; a main excretory duct which branches in to lobar ducts, interlobular ducts, and intralobular ducts.[15] The intralobular ducts consist of large striated ducts and small intercalated ducts.[12] The lumen of intercalated ducts is continuous with the acini which will be either spherical (serous) or tubular (mucous) in shape. Surrounding the terminal end pieces and intercalated ducts, the contractile myoepithelial cells are seen.[12] These cells are stellate in shape around the acini to help in expelling the saliva from the acini and fusiform in shape around the ducts to help in maintaining the patency of the duct lumens.[12]

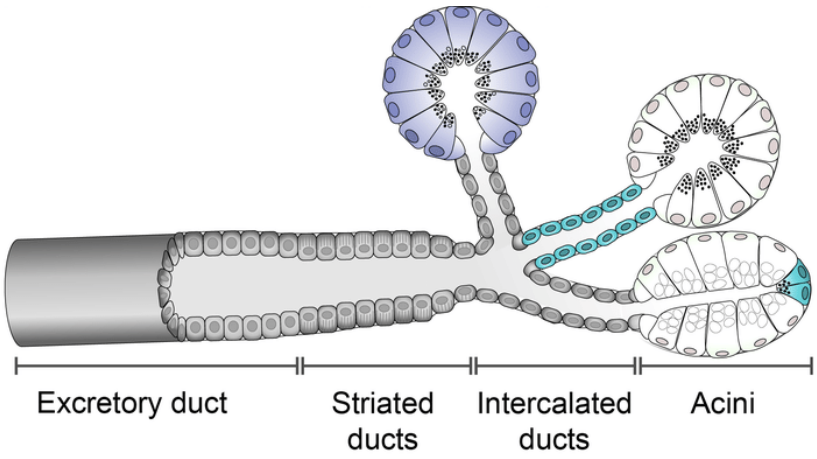

Figure 8: Ductal pattern of salivary glands

For all the major salivary glands, the main excretory duct is lined with epithelium that ranges from stratified squamous towards the oral cavity to pseudostratified columnar near the lobar ducts.[12]

The lobar ducts are lined with epithelium that may be high columnar to stratified cuboidal, while interlobular ducts are lined with high columnar epithelium.[15] The intralobular ducts and terminal end pieces differ for each salivary

gland. The terminal end pieces of the parotid glands are all spherical and of the serous type.[12]

Intercalated ducts are numerous and long in the parotid glands and they are lined with cuboidal epithelium with round central nuclei and sparse cytoplasm. Striated ducts, however, are lined with columnar epithelium with centrally located nuclei.[12]

In submandibular salivary gland, the intercalated and striated ducts are structurally similar but are less numerous than those found in the parotid gland.[12]However in sublingual gland both the intercalated and striated ducts are fewer and shorter in comparison with the parotid and submandibular glands.[12]

C. PHYSIOLOGY OF SALIVARY GLANDS:

The main function of salivary glands, both major and minor, is to produce saliva.[12] Parotid glands, being the largest salivary glands produce a significant amount of the total saliva volume (approximately 45% or 450 to 675 mL/day).[13] The saliva from the parotid is serous in nature, rich in amylase and glycoproteins.[12] Submandibular glands are the second largest salivary glands and they secrete approximately 45% of the total saliva volume.

The saliva secreted by submandibular salivary glands are more mucinous in nature. Sublingual glands contribute 5% of the total saliva volume (50 to 75 mL/day) and secrete saliva that are viscous in nature. Minor salivary glands also contribute about 5% of the total saliva volume but their saliva is purely mucinous and rich in secretory immunoglobulin A (IgA).[12,13] Hence, the saliva found in the oral cavity is termed mixed or whole saliva because it is composed of various

amounts of all these saliva types mixed with desquamated oral epithelial cells, microorganisms and their products, serum components along with inflammatory cells.[12]

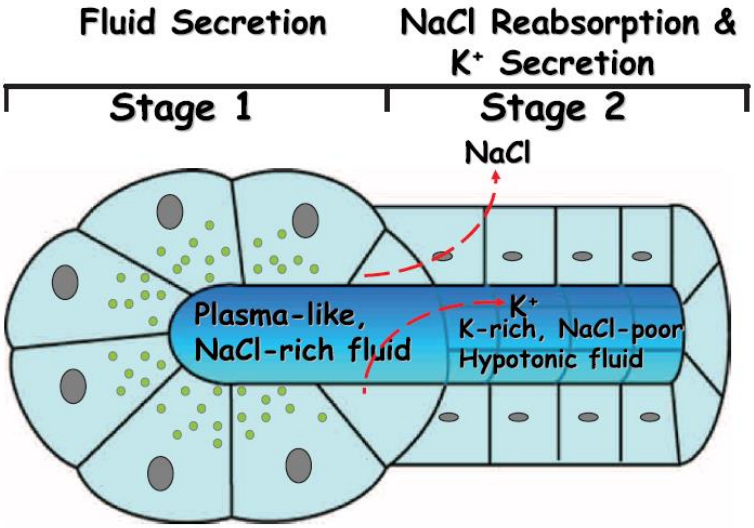

Figure 9: Physiology of major salivary gland

Production of saliva takes place within the acini. This primary saliva produced by the acinar cells are isotonic, high in sodium and low in potassium.[13] Saliva then undergoes modification in the striated ducts where sodium is reabsorbed and potassium is excreted, making it hypotonic.[12,13]

Saliva is predominantly made up of water (99.5%) with a specific gravity of 1.002 to 1.012.2 The production of saliva, especially from the major salivary glands, is under the control of the autonomic nervous system and is prompted by stimulation.[15] Therefore, more saliva is produced during the day when there is more chemical, mechanical, and olfactory stimulation with a total of approximately 1 to 1.5 L of saliva produced in 24 hours.[12]

D. FUNCTIONS OF SALIVA:

The functions of saliva are listed below.[12,16]

FUNCTION	EFFECT	ACTIVE SUBSTANCE
Protection	Mechanical washing Barrier	Water Mucin
Buffering	Neutralize acids Increase the pH	Bicarbonate and phosphate Urea and Ammonia
Antimicrobial	Antibodies Antibacterial Antifungal	Mucin Secretory IgA Lysozyme, Peroxidase Histatin
Tooth integrity	Enamel maturation Enamel remineralisation	Calcium, phosphate Fluoride
Taste	Dissolve substances Maintain taste buds	Water, Lipocalins Epidermal growth factor, Carbonic anhydrase VI
Digestion	Form food bolus Digest starch and triglycerides	Water, Mucin Amylase, Lipase
Tissue repair	Promote wound healing and clot formation	Growth factors Trefoil proteins

Table 1: Functions of Saliva

E. IMAGING OF SALIVARY GLANDS:

Salivary gland disorders comprise of a small yet an important group of head and neck pathologies ranging from salivary gland calculi to salivary gland tumors. There are various imaging techniques available towards the diagnostic approach of salivary gland disorders, which are listed below;[6,17,18]

- Plain radiography
- Ultrasonography
- Computed tomography (CT)
- Cone Beam Computed Tomography (CBCT)
- Magnetic resonance imaging (MRI)
- Radionuclide imaging
- Sialography (conventional, CT, CBCT, MRI)

PLAIN RADIOGRAPHY:

Plain radiography is the simplest, earliest, and cheapest way of studying the salivary glands. It is useful in detecting ductal calculi, and adjacent osseous lesions. Only a few of the salivary ductal calculi are radiolucent which cannot be appreciated by means of plain radiography.[19]

Parotid Gland: Antero-Posterior (AP), Lateral Oblique and Panoramic view (Puffed chin)

Submandibular Gland: Occlusal, Lateral Oblique and Panoramic view.[20]

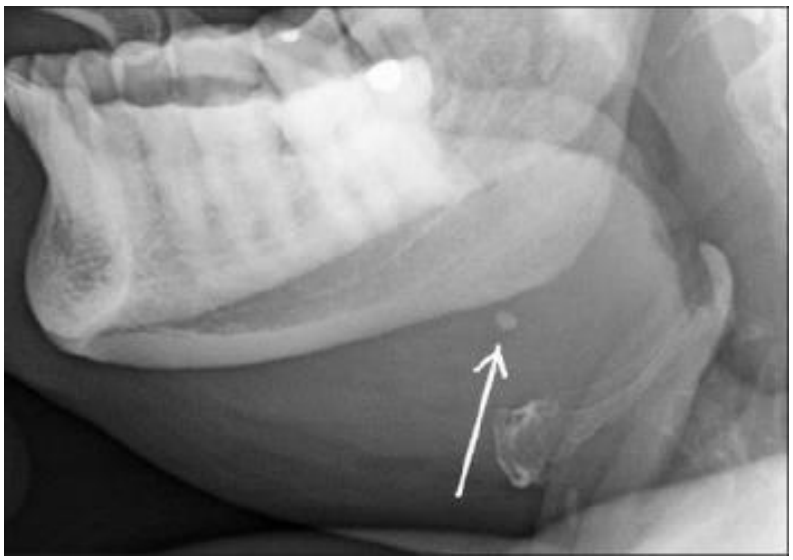

Figure 10: Plain radiograph of the submandibular region showing small calculus

Plain films whether intraoral or extraoral radiographs provide a relatively quick and inexpensive way to demonstrate calcified sialoliths. The clinical applicability of projection radiography, however is limited because only moderately sized and fairly dense calcifications can be identified.[5,13]

ULTRASONOGRAPHY:

It is a quick and noninvasive method of evaluating parotid and submandibular glands. Salivary glands appear homogeneously hyperechoic on ultrasonography. It is performed with a high frequency linear (7-10 MHz) transducer.[19] Now a days, the availability of high-resolution probes and harmonic imaging are available which help to delineate location, shape and margins of salivary neoplasms.[20] Ultrasonography helps in differentiating cystic lesions from that of solid lesions and also aids in guiding the exact site of Fine Needle Aspiration Cytology (FNAC) in suspected salivary gland pathologies.[21] Fine Needle Aspiration Cytology (FNAC) combined with color Doppler imaging, helps in estimating the blood flow within the lesion (malignant lesions of salivary glands are highly vascular as compared to their benign counterparts).[22,23] However, its diagnostic accuracy with regards to identifying sialoliths is still low. The major shortcoming of US is its inability to penetrate deep tissues.[5,13]

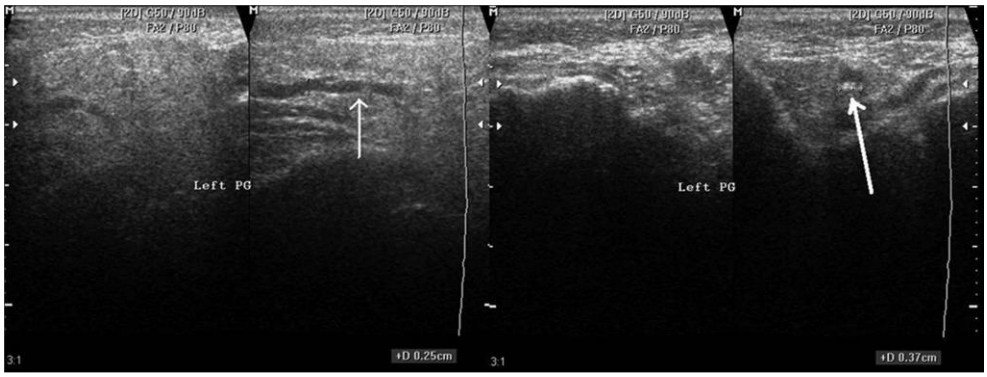

Figure 11: US images show altered echo pattern of the parotid gland with ductal dilatation (thin arrow) and small calculus (thick arrow) at its terminal end

COMPUTED TOMOGRAPHY:

Computed Tomography (CT) is an excellent imaging modality for evaluating the major salivary glands especially when an intravenous contrast medium is administered.[5] It is regarded by many as the modality of choice for imaging inflammatory conditions of these salivary glands.[13] Computed tomography also has a sensitivity of nearly 100% for detecting masses and the anatomical destruction created in the major salivary glands and also in its associated surrounding structures. Unfortunately, CT alone cannot differentiate benign from malignant masses because benign masses have capsules that give them a smooth well-defined contour when imaged and low grade malignancies have pseudocapsules that can also give them a smooth well-defined outline.[13] Fortunately, when CT findings are combined with clinical findings, the distinction between benign and malignant masses can be made in 90% of cases. With regard to obstructive conditions, CT demonstrates large calcified sialoliths with great sensitivity but fails to demonstrate small and non-calcified ones and it fails to show the ductal changes and soft tissue abnormalities that result from chronic obstruction.[13]

Figure 12: Non-contrast axial CT image showing submandibular sialolithiasis on right side (white arrow) and normal gland on left side

CONE BEAM COMPUTED TOMOGRAPHY:

Cone Beam Computed Tomography (CBCT) is the latest imaging modality used widely in maxillofacial radiology due to its high resolution, fast scanning time, low radiation dose and geometrically accurate images.[9,24] Due to the cone-shaped x-ray beam and two-dimensional detectors, the CBCT scanner can collect volume data by means of a single rotation taking 9-40 seconds.[10] The CBCT scanners provides better visualization of the maxillofacial region and evaluation of bony morphology. Combining the benefits of the CBCT with the versatility of the sialography would complement each other and can help in better visualization of the ductal architecture.[25]In fact CBCT sialography has proved to be superior to other imaging modalities in identifying non-calcified sialoliths which were usually difficult to detect and diagnose using other techniques.[1] It is promising because of the high correlation in interpreting the salivary gland lesions between the observers in terms of presence of stenosis, dilatation and evagination.[1,25]

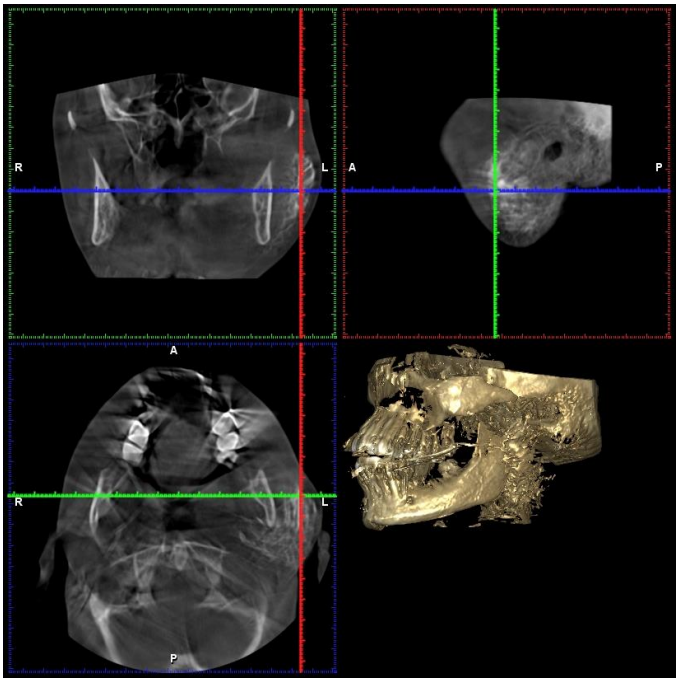

Figure 13: CBCT sialography showing normal parotid gland architecture in multiplanar view

MAGNETIC RESONANCE IMAGING:

Magnetic resonance imaging (MRI) is a non-invasive technique with advantages of superior soft tissue discrimination and multiformatted image visualization facility. MRI does not use ionizing radiation, so images can be obtained without any radiation harm to the patient. It also eliminates streak artifacts from dental restorative material, and is better to differentiate benign from malignant masses because of its superior soft tissue contrast resolution.[5,13] Malignancies of the salivary glands for example are more cellular and dense than benign lesions, and thus have low to intermediate signal intensities on all MRI sequences. In contrast, benign masses have a higher water content and thus a lower T1 signal intensity and a higher T2 signal intensity.[13] Signal changes in T1 and T2 weighted MR images are also helpful in cases of inflammation because they reflect the degree of edema versus infiltration by inflammatory cells.[13] Magnetic resonance imaging however, is not the imaging modality of choice for obstructive conditions of the salivary glands because of its low spatial resolution, long acquisition time, and the signal voids that are associated with calcified structures such as sialoliths.[26]

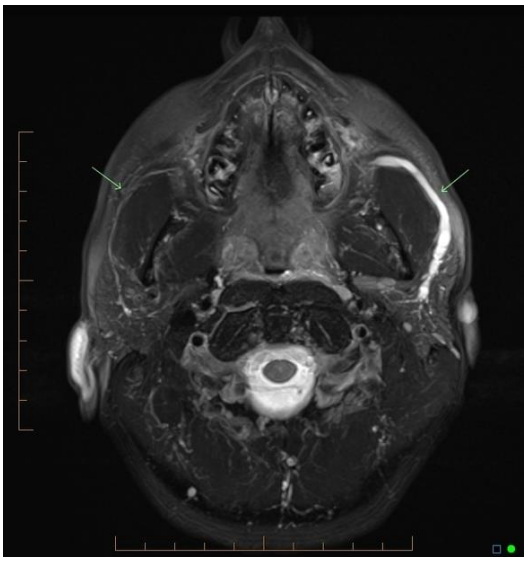

Figure 14: MRI image showing obstructed parotid salivary gland on right side

RADIONUCLIDE IMAGING:

Scintigraphy, is a functional imaging technique of the major salivary glands.[5,13] Unlike the previously mentioned imaging techniques, scintigraphy is a radiologic examination that does not examine the morphologic anatomy but rather the physiologic and metabolic function of a tissue or organ.[5] Scintigraphy uses a radioactive molecule that emits gamma rays which when injected intravenously, distributes in the body and is selectively concentrated in certain tissues. Later, it starts to decay emitting gamma rays which will be captured by a gamma camera.[13] Glandular tissues including the thyroid and salivary glands uptake, concentrate, and excrete the radiopharmaceutical technetium-99m (99mTc) pertechnetate (TPT). Technetium-99m (99mTc) is a metastable isotope of technetium with a short half-life of 6 hours, and pertechnetate is the water soluble ion that carries and distributes it in the body. In the salivary glands the concentration of TPT reaches a maximum at about 30 to 45 minutes.[5] Lesions are assessed either as an increased or decreased or nil uptake. Scintigraphy of the salivary glands like all other nuclear medicine imaging studies has high sensitivity but low specificity which in addition to its low resolution, limits its clinical applicability.[5]

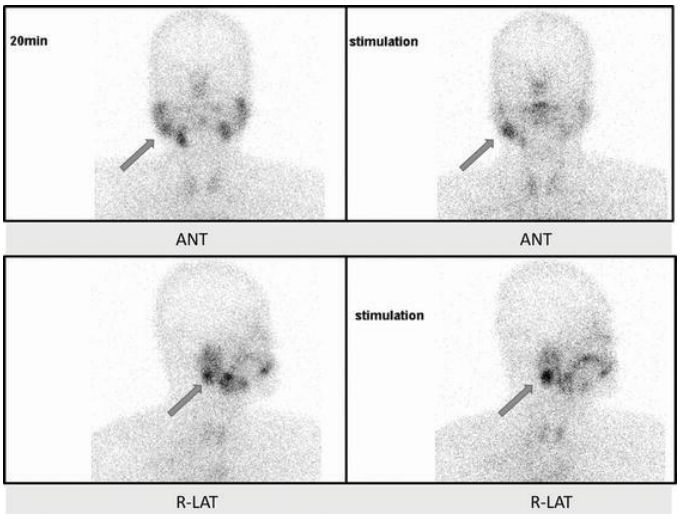

Figure 15: Scintigraphy - 20 minutes after administration, the radionuclide is taken up by the right parotid gland. The diagnosis was Warthin's tumor.

Positron emission tomography (PET) imaging is another radionuclide imaging technique, which uses radiotracers, which subsequently decay, with the emission of positively charged particles (positrons). These positrons travel a few millimetres in tissue before combining with negatively charged electrons, converting mass into energy and releasing two high energy (511 keV) photons (gamma rays) which are emitted at approximately $180^0$to each other. The simultaneous detection of these positrons by opposing detectors is then used to construct a three dimensional image of all these events known as PET image.[27] The main application of PET is the assessment of patients with cancer using the glucose analogue 2-[18] fluoro- 2-deoxy D-glucose (FDG) since the cancer cells have increased glucose utilization.[5]

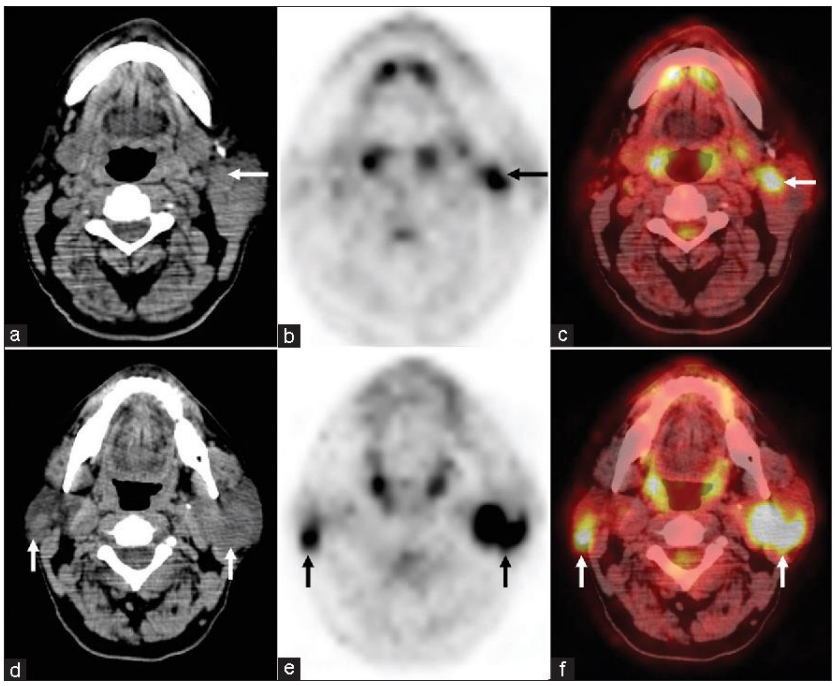

Figure 16: Axial positron emission tomography images (b and e) showing intense flourodeoxy glucose uptake in the parotid region corresponding to multiple soft tissue nodules in both the parotid glands seen on axial computed tomography

F. SIALOGRAPHY:

Sialography is the radiographic method of visualization of the major salivary glands following instillation of soluble contrast material into the ducts.[28,29] Sialography was first performed by Carpy in the year 1902 and it is one of the oldest techniques recorded in the literature.[20]

Sialography is indicated for evaluation of the intrinsic and/ or acquired defects of the salivary glandular ductal system as it provides a clear visualization of the branching ducts and acinus. The contraindications to sialography are active infection and allergy to contrast media.[5]

Initially, a scout radiograph will be taken. Following the radiograph, a high viscosity, water or oil soluble contrast agents that allow better visualization of the ductal structures will be injected inside the duct via the orifice. The gland is again imaged with the contrast agent within the gland.

Phases of imaging

- Preliminary plain film
- Injection / filling phase film
- Post evacuation / parenchymal phase film

Sialography can also be combined with MRI and CT, which is useful for determining the outer extent of large tumors, extra glandular extension, and the actual depth of such tumors.[20,30]

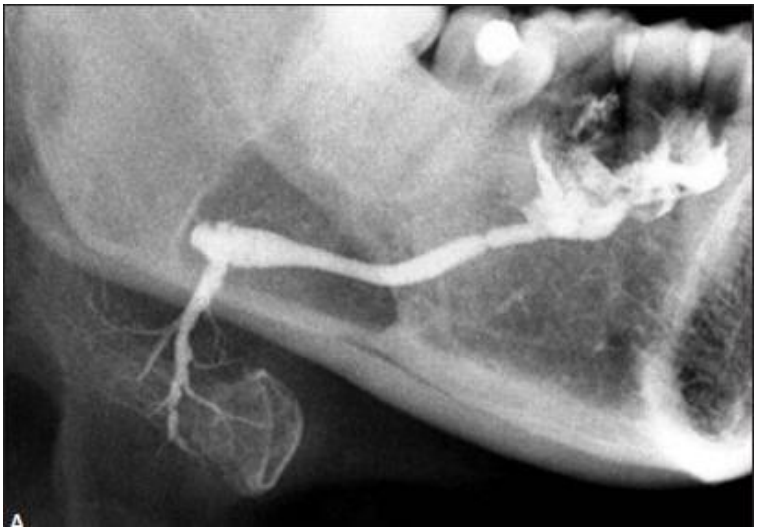

Figure 17: Submandibular salivary gland sialography showing ductal architecture

G. STUDIES RELATED TO 2D SIALOGRAPHY:

Ericson in 1971 studied the relation between the size of the parotid gland and the output of saliva in 92 healthy individuals of both sexes and of various ages. The size of the gland has been determined on sialograms and the secretions are estimated by sialometry were compared and evaluated. He concluded that the size of the gland and the difference in secretion is not associated with each other, but varies between different stimuli.[31]

Heun et al in 1972 on his study with 158 sialograms done on 126 patients evaluated the diagnostic criteria in various abnormalities of the major salivary glands and stated that sialography is a valuable diagnostic tool in the workup of pathologic conditions of the major salivary glands.[32]

Rose et al in 1950 assessed the effectiveness of sialography in diagnosis of salivary gland pathologies. The study included subjects with both normal salivary gland and also those with pathologies. Initially, patient history was taken along with clinical examination followed by sialography. The appearance of the ductal

architecture were compared and studied. The study proved that sialography was more reliable and effective in the diagnosis of salivary gland pathologies as well as in the visualization of the ductal architecture. They also added up stating that sialography is an important diagnostic tool in the detection of intraglandular and extraglandular swellings.[33]

Verhoeven et al in 1984 studied contrast media that are been used for sialography Eleven radiopaque substances were selected, and their properties were analyzed. An in vitro study was performed to determine their contrast qualities and their rate of evacuation after the sialographic examination. Moreover, the effects of the radiopaque material on the extraglandular tissues, which are vital in understanding the consequences of spilling into these tissues were investigated. The results of this study were compared with data from the literature. Conray 80, Amipaque 440, Lipiodol UF, Myodil, and Duroliopaque appear to be the media most suited for sialography, provided glandular overfilling is avoided.[34]

Daniels et al in 1996 studied the effectiveness of detecting the salivary component of Sjogren's syndrome. The study included patients with Sjogren's syndrome and sialography was carried over these patients. They compared the results with that of normal subjects. Later, the results obtained were evaluated and analysed with sialometry and salivary gland biopsies. They stated that Sialography appears to be diagnostically less sensitive but more specific than sialometry and more sensitive but less specific in comparison with salivary gland biopsies.[35]

Schortinghuis et al in 2009 did a study to assess the prevalence of lipiodol retention after parotid sialography. Archival images of 565 patients who had underwent sialography with lipidiol as contrast medium were collected and

evaluated. Based upon the results, they concluded that patients who had lipidiol as contrast agent in sialography had minimum adverse effects.[36]

Sujatha et al in 2009 studied the efficacy of sialography with three patients affected by inflammatory salivary gland disease and concluded that Sialography remains the most popular imaging procedure for assessment of ductal inflammatory and degenerative diseases despite the more sophisticated imaging techniques currently available. Sialography also proved to be a therapeutic aid in cases of obstructive sialadenitis and recurrent infections.[37]

Wangyonget al in 2016 aimed to identify if the existence of the accessory parotid gland correlated with the etiology of parotitis. Sialographic data of affected individuals were compared with that of normal individuals. The study concluded that the accessory parotid gland might play a role in the pathogenesis of parotitis. The existence of an accessory parotid gland is likely to interfere with salivary flow. Computational fluid dynamics analysis of salivary flow in the ductal system would be useful in future etiologic studies on parotitis.[38]

Wu et al in 2017 studied the role of sialography in the diagnosis of chronic parotitis. They included 142 patients with chronic parotitis who underwent sialography from January 2014 to January 2016. Among the subjects, 88 patients with chronic obstructive parotitis, 21 with chronic obstructive parotitis related to Sjögren's syndrome, 9 children with chronic recurrent parotitis, 11 with radioactive iodine induced parotitis, 13 with chronic obstructive parotitis related to diabetes were evaluated. All of them underwent sialography along with sialendoscopy. The findings of both the studies were compared in order to signify the diagnosis of chronic parotitis. Based upon the results the concluded that sialography was more

specific in comparison with sialoendoscopy and prove to be more effective in the identification of chronic parotitis.[39]

Tucci et al in 2019 studied the Diagnostic and Therapeutic Effectiveness of Sialography with a Retrospective Study on 110 children for over a period of 10 years who were been affected by juvenile recurrent parotitis**.** By evaluating the degree of episodes of parotid swelling before and after sialography, the Outcome of the procedure was measured. Based upon the study, the concluded that sialography is a reliable method in the diagnosis of juvenile recurrent parotitis. They also stated that sialography is also an effective therapeutic procedure which yield importance in the treatment of juvenile recurrent parotitis. Sialography is a method that can be even carried out in normal setting, without the use of anaesthetic agent and it also proves to be cost effective and minimum complicative procedure.[40]

H. STUDIES RELATED TO 3D SIALOGRAPHY:

Hansson et al in 1987 conducted a study on 59 patients to compare the effectiveness of plain sialography and computed tomography sialography. The study comprised of patients who were been suspected of having neoplasms in the major salivary glands. CT sialography and conventional sialography were assessed and evaluated. They concluded that the valuable advantage of parotid CT sialography in comparison with conventional sialography is the ability of evaluating the neoplasm in its actual form and size along with its effects on adjacent structures and they also stated that computed sialography had the ability to delineate the ductal architecture, empowering the better visualization of ductal pattern .[41]

Kalinowski et al in 2002 studied the diagnostic accuracies of MR sialography and digital subtraction sialography in patients with successful completion of both examinations in 80 patients and concluded that MR sialography serves as essential tool in visualization of parotid and submandibular salivary glands. Digital subtraction sialography on the other hand, has a substantial procedural failure rate, although being an invasive technique. It is more commonly used for imaging of submandibular duct. However, because of its superior spatial resolution, it plays an important role in diagnostic radiology in comparison with that of MR sialography.[30]

Jadu et al in 2010 compared conventional sialography and cone beam computed tomography sialography by taking their effective radiation doses into concern, in imaging of both parotid and submandibular salivary glands. The effective doses were been evaluated from 25 selected locations in the head and neck with a help of a radiation analogue dosimeter (RANDO) phantom, which is based upon the criteria given by International Commission on Radiological Protection 2007. The study concluded that the effective doses of CBCT at 15 cm FOV with 80 kVp and 10 mA is similar to that of the effective dose of conventional sialography in imaging of both the parotid and submandibular salivary glands.[42]

Wahed et al in 2013 included eight patients, who are suspected victims of major salivary gland disorders in order to access the effective role of cone-beam computed tomography sialography imaging in the detection of major salivary gland pathologies. Conventional sialography images were taken using orthopantomography and lateral oblique radiography along with CBCT sialography. Three blinded radiologists manipulated and assessed the images separately. Analysis

of the results proved higher interobserver correlation between the radiologists in the detection of various ductal and glandular abnormalities. However, CBCT sialography proved its worthiness over the other conventional imaging in the better visualization of ductal architecture along with the detection of salivary gland abnormalities.[25]

Jadu et al in 2013 did a study with 47 patients who underwent both conventional imaging and CBCT imaging of either parotid or submandibular gland sialography over a period of two years. The diagnostic abilities of conventional sialography were compared with that of two cone beam computed tomography sialography. Three blinded radiologists manipulated and assessed the images separately. The study proved the better appreciation of glandular pattern and calculi detection with the help of three dimensional cone beam computed tomography sialography. The high negative per cent agreement for strictures suggests that, if strictures are identified on CBCT images, then obstruction can be ruled in.[1]

Shahidi et al in 2014 studied the effectiveness of Cone beam computed tomography (CBCT) three cases to confirm its feasibility and superiority. The study stated that conventional sialography is not diagnostic whereas MRI and CT are not of easy accessibility or else affordable, but CBCT sialography and its 3D images are feasible and are very much helpful in diagnosis of major salivary gland disease.[43]

Kroll et al in 2015 studied the use of CBCT sialography in the detection of salivary gland pathologies within the intra glandular duct system when ultrasound was inconclusive. The study comprised of 14 subjects suffering from recurrent swelling of a major salivary gland for whom CBCT images were taken. Four blinded radiologists evaluated the acquired data independently. Three of the detected

pathologies were strictly intraglandular. The study concluded that CBCT sialography showed a promising supplementary non-invasive diagnostic tool for the better visualization of the intraglandular ductal pattern of the both parotid and submandibular salivary glands.[44]

Chellathurai et al in 2016 in their study compared the accuracy of the conventional sialography in comparison with MR Sialography in the diagnosis and detection of major salivary gland abnormalities. The study included 54 subjects diagnosed with non-tumorous salivary gland pathologies. The accuracy of diagnosis of plain sialogram and MR Sialogram was studied in comparison with that of clinical data. The study provided a positive correlation between MRI features and the data obtained clinically. Hence by the study proved that, MRI is extremely efficient in the detection of salivary gland abnormalities.[45]

Bertin et al in 2017 studied the effectiveness of three-dimensional CBCT (3DCBCT) sialography in assessing non-tumour salivary gland diseases. The study comprised of 60 patients with parotid or submandibular salivary symptoms for whom CBCT images were taken. Images were processed with multiplanar and 3D reconstructions. Based upon the study, they concluded that 3D-CBCT sialography seems to serve as are liable tool of diagnostic value for the study of salivary gland ductal diseases.[46]

MATERIALS AND METHOD

MATERIALS AND METHODS

A. SOURCE OF DATA:

The study was planned and carried out in the Department of Oral Medicine and Radiology, Sree Mookambika Institute of Dental Sciences, Kulasekharam to evaluate the effectiveness of Cone Beam Computed Tomography Sialography in diagnosing salivary gland lesions.

B. METHODS OF SELECTION OF DATA:

Sample size:

- Total number of samples: 25

Detailed description of the Samples:

Consists of CBCT sialography images with parotid and submandibular gland pathologies satisfying the inclusion criteria.

C. SELECTION OF CASES:

Inclusion criteria:

- Archival CBCT sialography images with salivary gland pathologies.

Exclusion criteria:

- CBCT images sialography which are technically imperfect.

Parameters to be studied:

Evaluation of normal and abnormal structures in the parotid and submandibular glands in CBCT sialography images.

D. ARMAMENTARIUM:

- OnDemand 3DTM software
- Sircona Galaxis Galileos software
- CBCT interpretation algorithm.

ALGORITHM TO BE FOLLOWED:

Normal Features

I. Primary Duct

1. Visualization: 0 1 2 3

    0-Not present

    1-Not Clearly Seen

    2-Clearly Seen

    3-Imaging Irregularities

2. Presence of Abnormalities: 0 1 2 3

    0-Not Present

    1-Not Sure

    2-Probably Present

    3-Definitely Present

II. Secondary Duct

3. Visualization: 0 1 2 3

    0-Not present

    1-Not Clearly Seen

    2-Clearly Seen

    3-Imaging Irregularities

4. Presence of Abnormalities: 0 1 2 3

0-Not Present

1-Not Sure

2-Probably Present

3-Definitely Present

III. Parenchyma

5. Visualization: 0 1 2 3

0-Not present

1-Not Clearly Seen

2-Clearly Seen

3-Imaging Irregularities

6. Presence of Abnormalities: 0 1 2 3

0-Not Present

1-Not Sure

2-Probably Present

3-Definitely Present

Abnormal features

I. Sialolith

7. Number: 0 1 2 3

0-Not Present

1-Solitary

2-Multiple

3-Sialolithiasis

8. Size: 0 1 2 3 4

    0-Nil

    1-Less Than 2mm

    2-Ranges between 2-4mm

    3-Ranges between 4-8mm

    4-More than 8mm

9. Location: 0 1 2 3

    0-Nil

    1-In the Primary Duct

    2-In the Secondary Duct

    3-Parenchyma

10. Obstruction: 0 1 2

    0-Not Present

    1-Partially Obstructed

    2-Fully Obstructed

II. Strictures:

11. Number: 0 1 2 3

    0-Not Present

    1-One Present

    2-Two Present

    3-Multiple Present

12. Location: 0 1 2 3

    0-Nil

    1-Within the Duct

2-Within Interglandular Second Order Branches

3-Elsewhere

13. Occludance: 0 1 2

0-Nil

1-Completely Occluding

2-Partially Occluding

III. Ductal Dilatation:

14. Cause: 0 1 2

0-Nil

1-Pathological

2-Imaging Characteristics

15. Severity: 0 1 2 3

0-Nil

1-Least Severe

2-Less Severe

3-Severe

IV. Acinar Pooling:

16. Number: 0 1 2

0-Not Present

1-Less than 1/3rd of the Gland Size

2-More than 1/3rd of the Gland Size

V. Mass:

17. Number: 0 1 2

    0-Not Present

    1-One Present

    2-More Than One Present

18. Borders : 0 1 2

    0-Nil

    1-Not Clearly Seen

    2-Clearly Seen

19. Internal Structures: 0 1 2

    0-Nil

    1-Not Clearly Seen

    2-Clearly Seen

20. Effect On Surrounding Structures: 0 1 2 3 4

    0-Nil

    1-Not Present

    2-Not Sure

    3-Probably Present

    4-Definitely Present

E. PROCEDURE IN DETAIL:

The study was carried out in the Department of Oral Medicine and Radiology, Sree Mookambika Institute of Dental Sciences. Twenty five CBCT sialography images which fulfill the inclusion and exclusion criteria were obtained from various CBCT centers. The images were been viewed in "Samsung Sync

Master SA100 Desktop with 4GB Graphics card". Later, the images were manipulated with the use of OnDemand 3DTM Project Viewer Limited Database Software (DICOM CD Database, Cybermed Inc., Seoul, Korea) and Sircona Galaxis Galileos V1.9 in multiplanar formatted image slices as well as 3D rendered formatted images to examine the lesions. Four blinded experts manipulated and evaluated the images independently and scores were given for the interpretation of the images according to the proposed algorithm. The algorithm for evaluation were been used by each radiologist to assess and interpret the CBCT images separately and then the results were been discussed with the others. Analysis of the results was done in order to appreciate the interobserver concordance among interpretations. Finally the results were tabulated in "Microsoft Excel" and was evaluated according to consensus and statistical analysis based on "Chi square test".

COLOUR PLATES

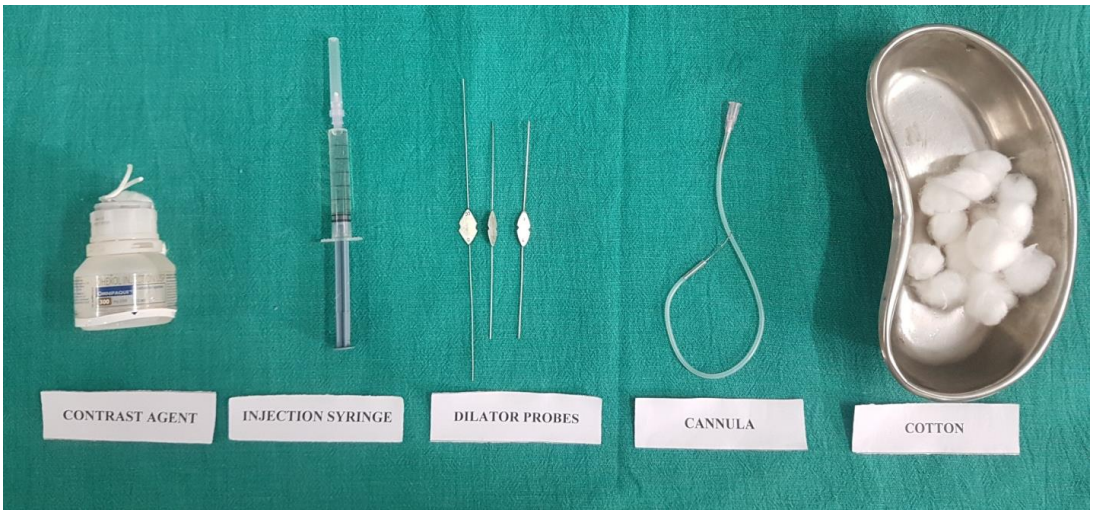

CP: 1 Sialography Kit

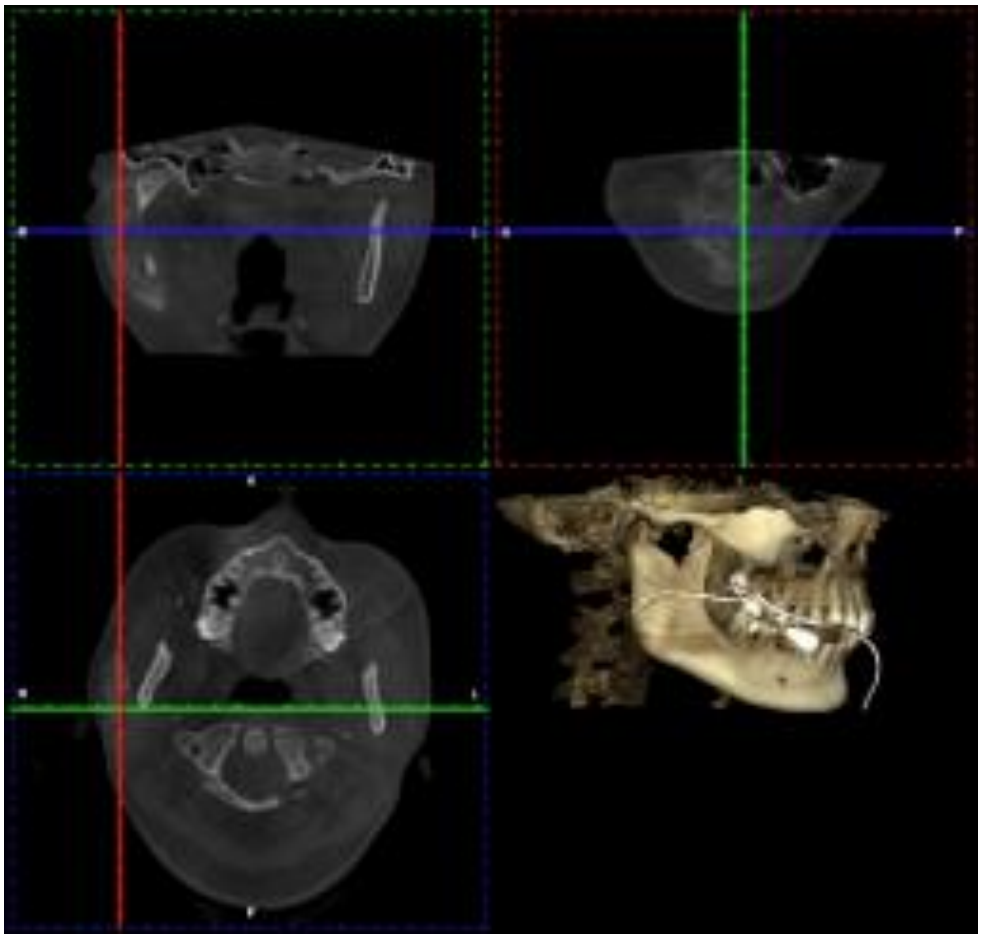

CP: 2 Multiformatted view of CBCT Sialography images

RESULTS AND OBSERVATION

RESULTS AND OBSERVATION

The study was conducted in order to evaluate the efficacy of cone beam computed tomography sialography in the detection of salivary gland lesions. A total of 15 CBCT images were included in the study and each images were assessed based upon an algorithm with 20 questions. Four blinded radiologists manipulated and evaluated the images separately. Statistical Package for Social Sciences (SPSS 16.0) version was used for data analysis. Chi square test was applied to find the statistical significance. A significance of p value less than 0.05 significant at 95% confidence interval was derived.

On comparison of interobserver variability on the visualization of primary duct between the four observers revealed concordance in observation.

Table-2: Comparison of primary duct visualization between four observers

Visualization	Observer I	Observer II	Observer III	Observer IV	p value
Not present	0	0	0	0	**-**
Not clearly seen	3	3	3	3	**0.86**
Clearly seen	12	12	12	12	**0.74**
Imaging irregularities	0	0	0	0	**-**

(p>0.05 no significant difference compared between observers)

On comparison of interobserver variability, upon the presence of abnormalities in the primary duct revealed, no significantstatistical difference in observation between the observers.

Table-3: Comparison of primary duct presence of abnormalities between four observers

Abnormalities	Observer I	Observer II	Observer III	Observer IV	p value
Not present	12	13	13	13	**0.89**
Not sure	2	2	2	2	**0.19**
Probably present	0	0	0	0	**-**
Definitely present	1	0	0*	0	**0.15**

(p>0.05 no significant difference compared between observers)

On comparison of interobserver variability on the visualization of secondary duct between the four observers revealed concordance in observation.

Table-4: Comparison of secondary duct visualization between four observers

Visualization	Observer I	Observer II	Observer III	Observer IV	p value
Not present	1	1	1	1	**0.84**
Not clearly seen	0	0	0	0	**-**
Clearly seen	14	14	14	14	**0.78**
Imaging irregularities	0	0	0	0	**-**

(p>0.05 no significant difference compared between observers)

On comparison of interobserver variability, upon the presence of abnormalities in the secondary duct revealed, no significant statistical difference in observation between the observers.

Table-5: Comparison of secondary duct presence of abnormalities between four observers

Abnormalities	Observer I	Observer II	Observer III	Observer IV	p value
Not present	14	12	14	14	**0.34**
Not sure	1	3	1	1	**0.19**
Probably present	0	0	0	0	**-**
Definitely present	0	0	0	0	**-**

(p>0.05 no significant difference compared between observers)

On comparison of interobserver variability on the visualization of parenchyma between the four observers revealed concordance in observation.

Table-6: Comparison of parenchyma visualization between four observers

Visualization	Observer I	Observer II	Observer III	Observer IV	p value
Not present	0	0	0	0	**-**
Not clearly seen	1	0	0	0	**0.14**
Clearly seen	14	15	15	15	**0.56**
Imaging irregularities	0	0	0	0	**-**

(p>0.05 no significant difference compared between observers)

On comparison of interobserver variability, upon the presence of abnormalities in the parenchyma revealed, no significant statistical difference in observation between the observers.

Table-7: Comparison of parenchyma presence of abnormalities between four observers

Abnormalities	Observer I	Observer II	Observer III	Observer IV	p value
Not present	7	6	8	6	**0.12**
Not sure	0	0	0	0	**-**
Probably present	0	0	0	0	**-**
Definitely present	8	9	7	9	**0.24**

(p>0.05 no significant difference compared between observers)

On comparison of interobserver variability, on the detection of number of sialolith in the included CBCT images revealed no significant difference in observation between the observers.

Table-8: Comparison of sialolith number between four observers

Number	Observer I	Observer II	Observer III	Observer IV	p value
Not present	14	15	15	15	**0.23**
Solitary	0	0	0	0	**-**
Two	1	0	0	0	**0.18**
Sialolithiasis	0	0	0	0	**-**

(p>0.05 no significant difference compared between observers)

On comparison of interobserver variability, on the evaluation of size of sialolith in the CBCT images revealed no significant statistical difference in observation between the observers.

Table-9: Comparison of sialolith size between four observers

Size	Observer I	Observer II	Observer III	Observer IV	p value
Nil	14	15	15	15	**0.23**
Less than 2 mm	1	0	0	0	**0.18**
2-4 mm	0	0	0	0	**-**
4-8 mm	0	0	0	0	**-**
More than 8 mm	0	0	0	0	**-**

(p>0.05 no significant difference compared between observers)

On comparison of interobserver variability, on the evaluation of location of the sialolith in the CBCT images revealed no significant statistical difference in observation between the observers.

Table-10: Comparison of sialolith location between four observers

Location	Observer I	Observer II	Observer III	Observer IV	p value
Nil	14	15	15	15	**0.23**
Primary duct	1	0	0	0	**0.18**
Secondary duct	0	0	0	0	**-**
Parenchyma	0	0	0	0	**-**

(p>0.05 no significant difference compared between observers)

On comparison of interobserver variability, on the assessment of location of the sialolith in the CBCT images revealed no significant statistical difference in observation between the observers.

Table-11: Comparison of sialolith obstruction between four observers

Obstruction	Observer I	Observer II	Observer III	Observer IV	p value
Not present	12	12	11	11	**0.29**
Partially obstructed	0	0	0	0	**-**
Fully obstructed	3	3	4	4	**0.23**

(p>0.05 no significant difference compared between observers)

On comparison of interobserver variability, on the presence of strictures in the CBCT images revealed no significant statistical difference in observation between the observers.

Table-12: Comparison of strictures number between four observers

Number	Observer I	Observer II	Observer III	Observer IV	p value
Not present	12	12	11	11	**0.29**
One	0	0	0	0	**-**
Two	3	3	4	4	**0.23**
Multiple	0	0	0	0	**-**

(p>0.05 no significant difference compared between observers)

On comparison of interobserver variability, on the location of strictures in the CBCT images revealed no significant statistical difference in observation between the observers.

Table-13: Comparison of strictures location between four observers

Location	Observer I	Observer II	Observer III	Observer IV	p value
Nil	12	12	11	11	**0.29**
Within the duct	0	0	0	0	**-**
Within Interglandular second order branches	3	3	4	4	**0.23**
Elsewhere	0	0	0	0	**-**

(p>0.05 no significant difference compared between observers)

On comparison of interobserver variability, on the evaluation of occludance of the strictures in the CBCT images proved to have no significant statistical difference in observation between the observers.

Table-14: Comparison of strictures occludance between four observers

Occludance	Observer I	Observer II	Observer III	Observer IV	p value
Nil	10	11	10	10	**0.27**
Completely occluding	0	0	0	0	**-**
Partially occluding	5	4	5	5	**0.43**

(p>0.05 no significant difference compared between observers)

On comparison of interobserver variability, on the cause of ductal dilatation in the CBCT images showed significant statistical difference in observation between the observers.

Table-15: Comparison of ductal dilatation cause between four observers

Cause	Observer I	Observer II	Observer III	Observer IV	p value
Nil	3*	9	9	9	**0.03**
Pathological	3	2	3	3	**0.45**
Imaging characteristics	9*	4	3	3	**0.05**

(*p<0.05 significant difference compared between observers)

On comparison of interobserver variability, on the detection of severity of ductal dilatation in the CBCT images showed significant statistical difference in observation between the observers.

Table-16: Comparison of ductal dilation severity between four observers

Dilation severity	Observer I	Observer II	Observer III	Observer IV	p value
Nil	5*	10	11	10	**0.04**
Least severe	6*	2	2	3	**0.04**
Less severe	3	2	1	2	**0.78**
Severe	1	1	1	0	**0.34**

(*p<0.05 significant difference compared between observers)

On comparison of interobserver variability, on the presence of acinar pooling in the CBCT images showed no significant statistical difference in observation between the observers.

Table-17: Comparison of acinar pooling number between four observers

Number	Observer I	Observer II	Observer III	Observer IV	p value
Not present	9	9	10	9	**0.34**
Less than 1/3rd of the gland size	6	6	5	5	**0.32**
More than 1/3rd of the gland size	0	0	0	1	**0.12**

(p>0.05 no significant difference compared between observers)

On comparison of interobserver variability, on the presence of space occupying mass in the CBCT images showed no significant statistical difference in observation between the observers.

Table-18: Comparison of mass number between four observers

Number	Observer I	Observer II	Observer III	Observer IV	p value
Not present	10	10	10	10	**0.89**
One present	3	5	5	5	**0.34**
More than one present	2	0	0	0	**0.17**

(p>0.05 no significant difference compared between observers)

On comparison of interobserver variability, to determine the borders of space occupying mass in the CBCT images showed no significant statistical difference in observation between the observers.

Table-19: Comparison of mass borders between four observers

Borders	Observer I	Observer II	Observer III	Observer IV	p value
Nil	10	10	10	10	**0.89**
Not clearly seen	0	0	0	0	**-**
Clearly seen	5	5	5	5	**0.85**

(p>0.05 no significant difference compared between observers)

On comparison of interobserver variability, to detect the ability of assessing the internal structures of space occupying mass in the CBCT images showed no significant statistical difference in observation between the observers.

Table-20: Comparison of mass internal structures between four observers

Internal structures	Observer I	Observer II	Observer III	Observer IV	p value
Nil	10	10	10	10	**0.89**
Not clearly seen	1	1	1	1	**0.45**
Clearly seen	4	4	4	4	**0.73**

(p>0.05 no significant difference compared between observers)

On comparison of interobserver variability, to determine the effect of space occupying lesions on the adjacent structures in the CBCT images showed no significant statistical difference in observation between the observers.

Table-21: Comparison of mass effect on surrounding structures between four observers

Surrounding structures	Observer I	Observer II	Observer III	Observer IV	p value
Nil	10	10	10	10	**0.89**
Not present	3	3	3	3	**0.45**
Not sure	1	1	1	2	**0.32**
Probably present	0	0	0	0	**-**
Definitely present	1	1	1	0	**0.19**

(p>0.05 no significant difference compared between observers)

Graph-1: Comparison of primary duct visualization between four observers

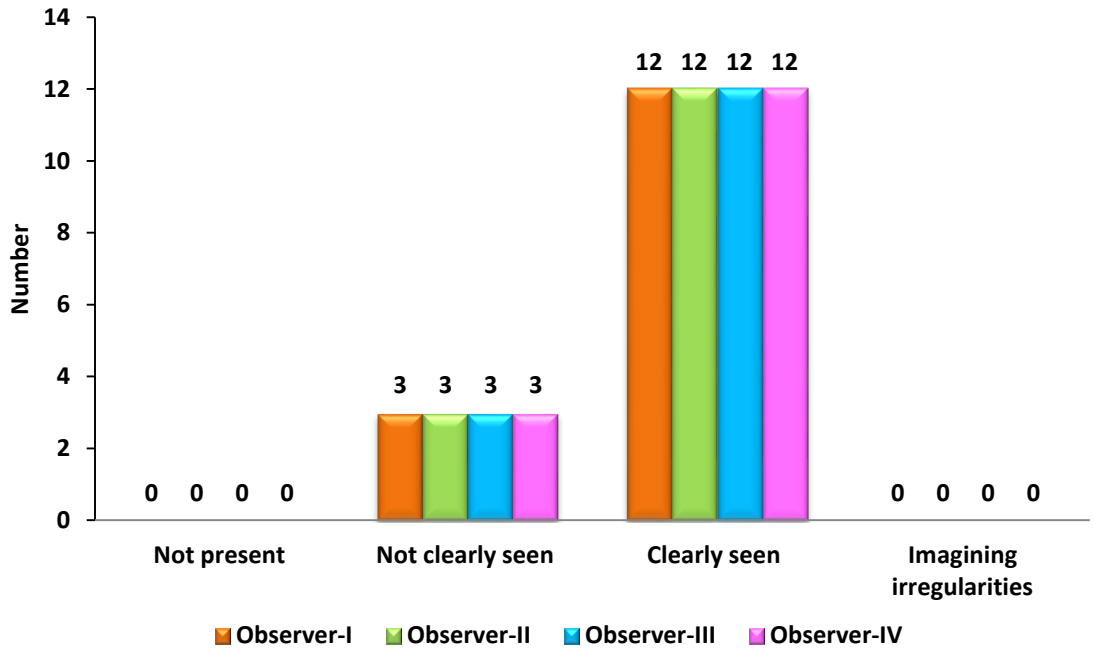

Graph-2: Comparison of primary duct presence of abnormalities between four observers

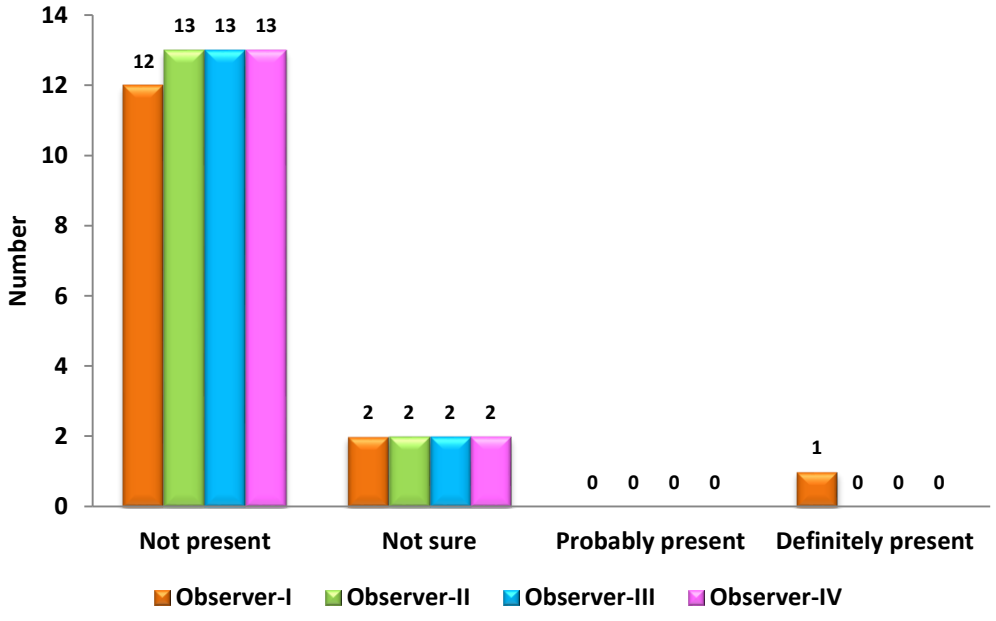

Graph-3: Comparison of secondary duct visualization between four observers

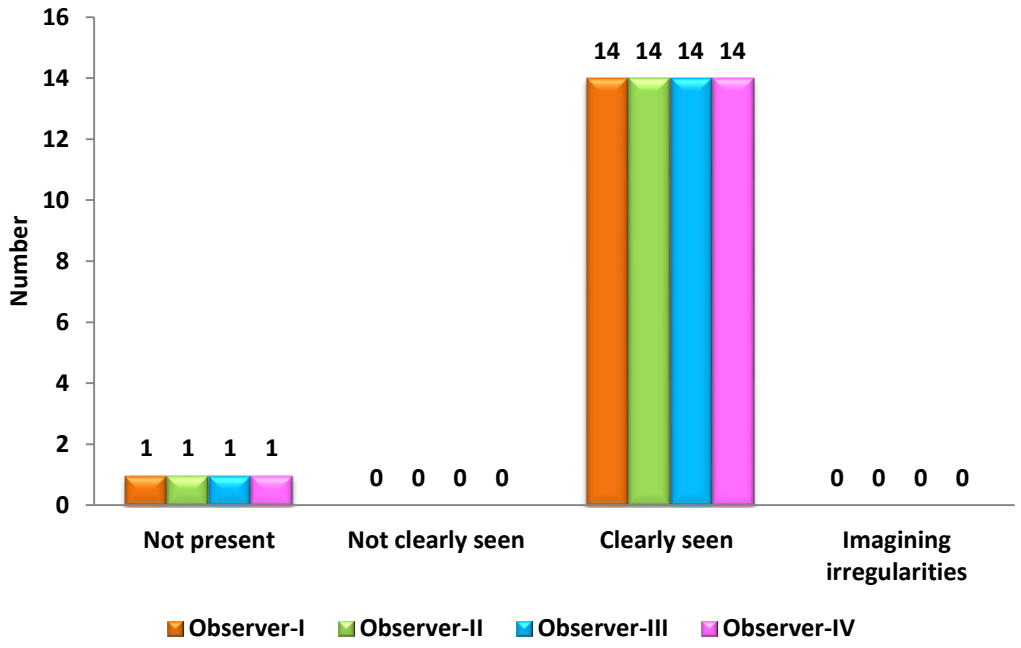

Graph-4: Comparison of secondary duct presence of abnormalities between four observers

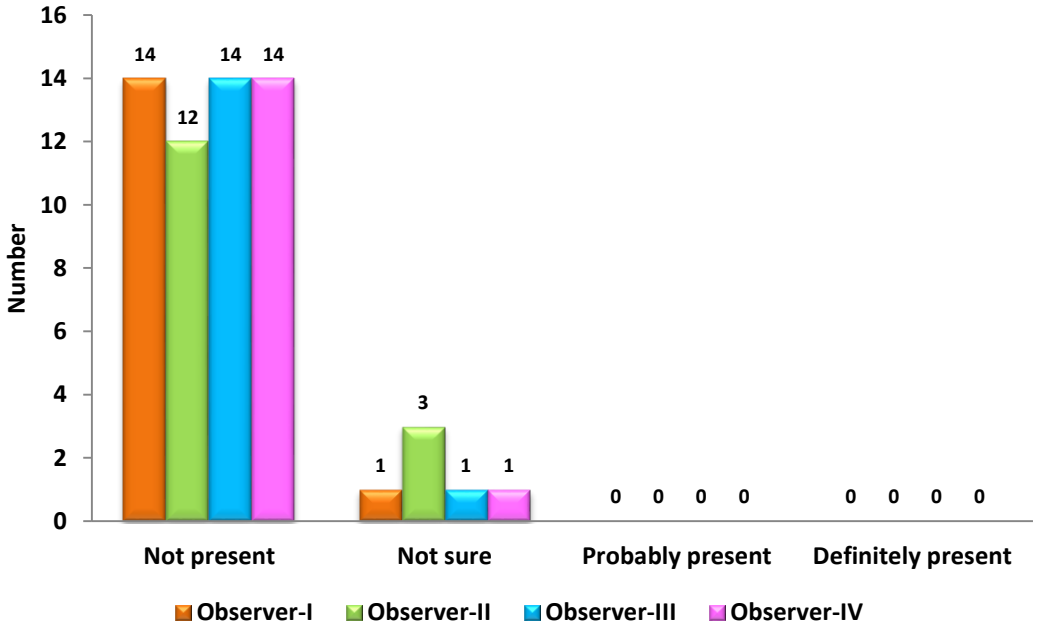

Graph-5: Comparison of parenchyma visualization between four observers

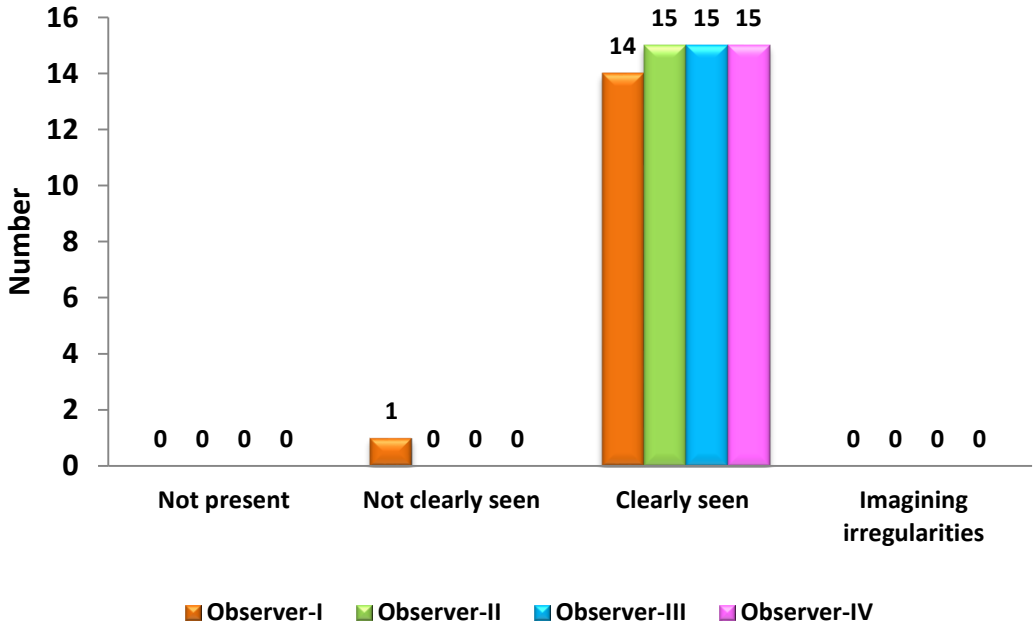

Graph-6: Comparison of parenchyma presence of abnormalities between four observers

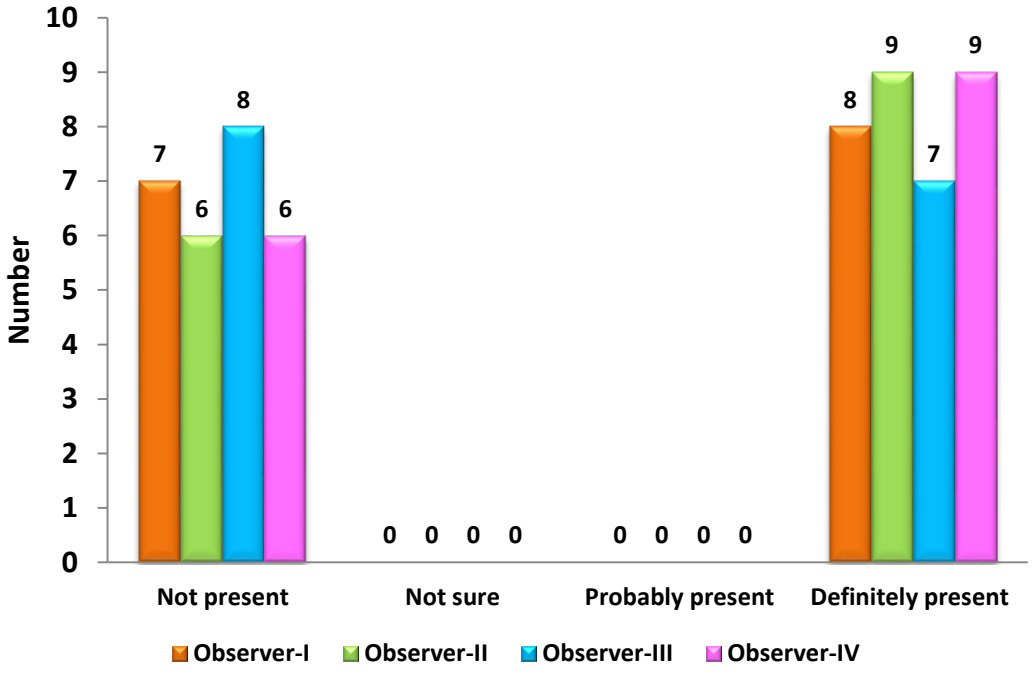

Graph-7: Comparison of sialolith number between four observers

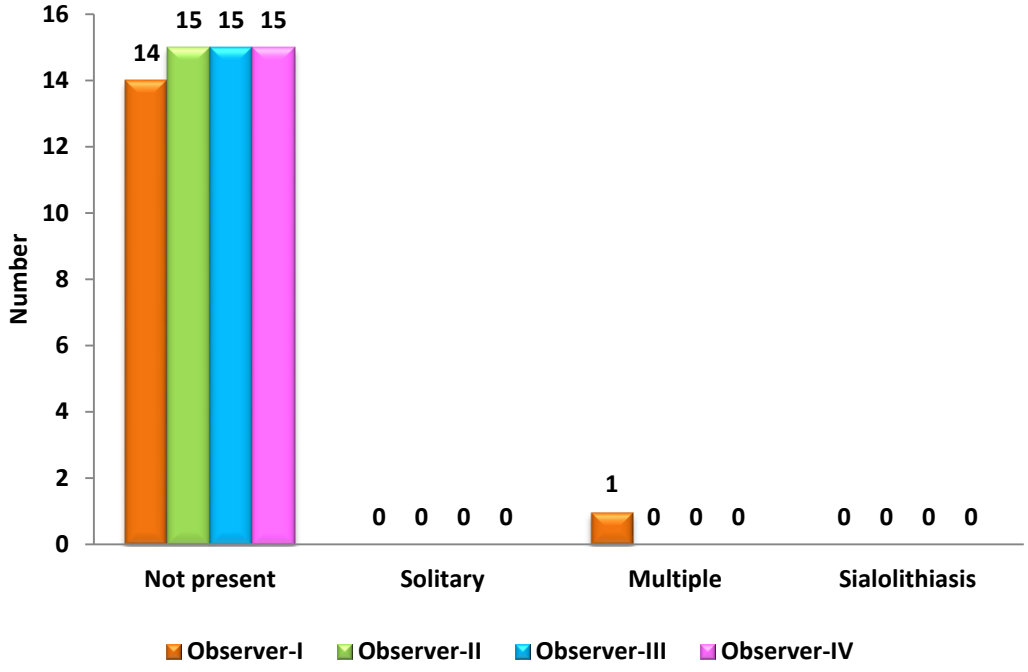

Graph-8: Comparison of sialolith size between four observers

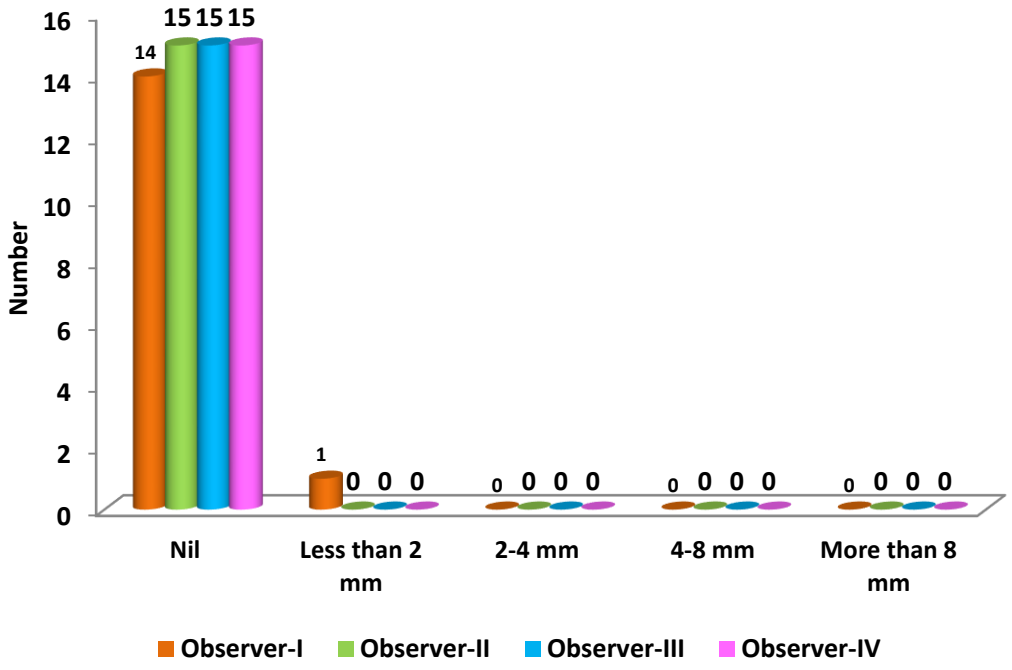

Graph-9: Comparison of sialolith location between four observers

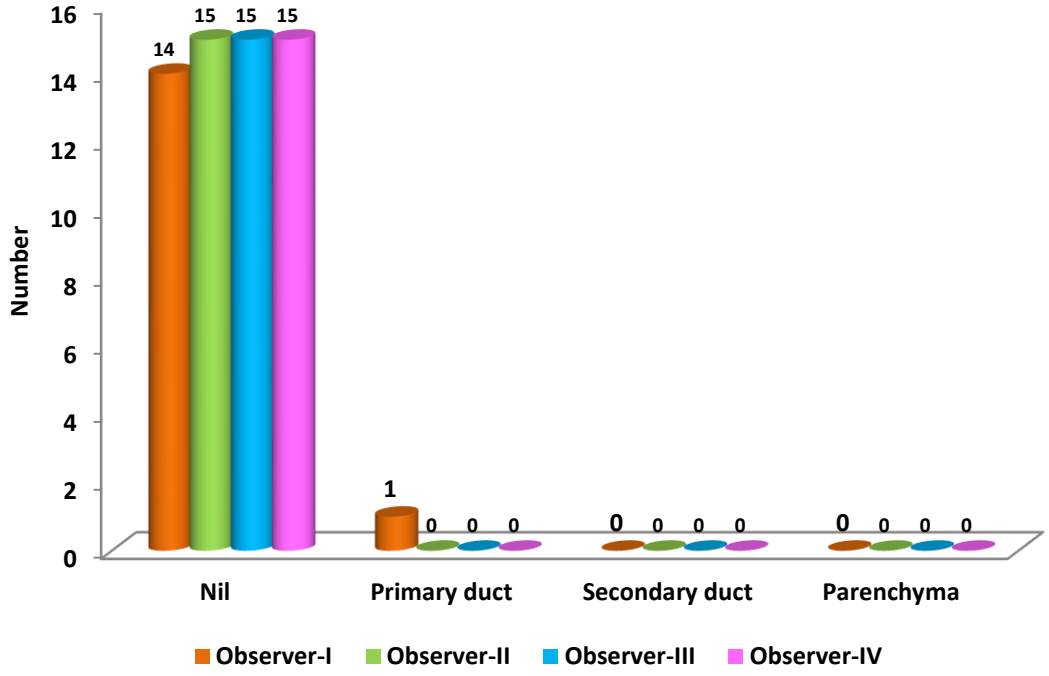

Graph-10: Comparison of sialolith obstruction between four observers

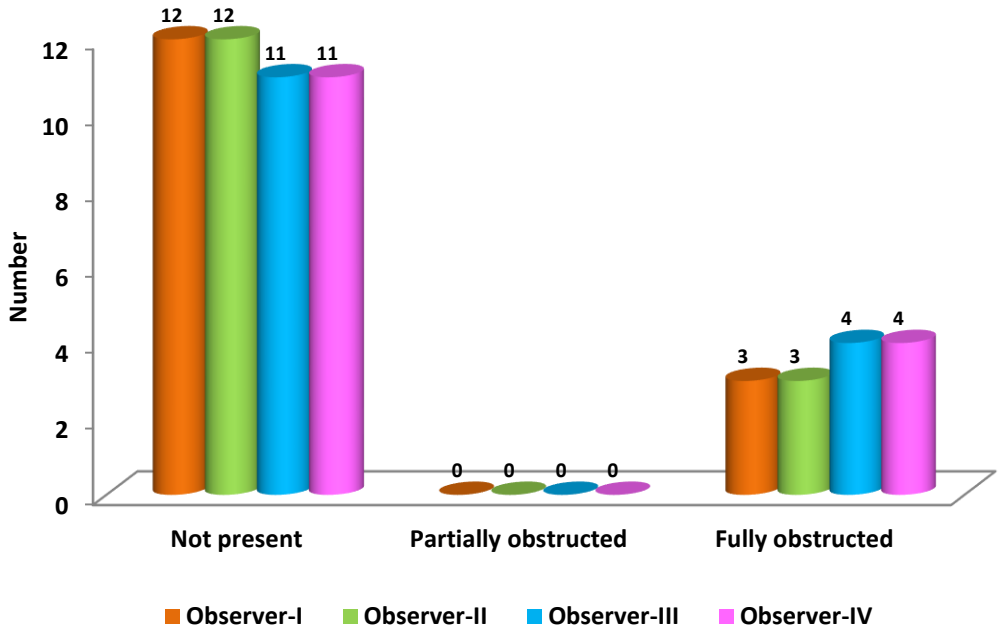

Graph-11: Comparison of strictures number between four observers

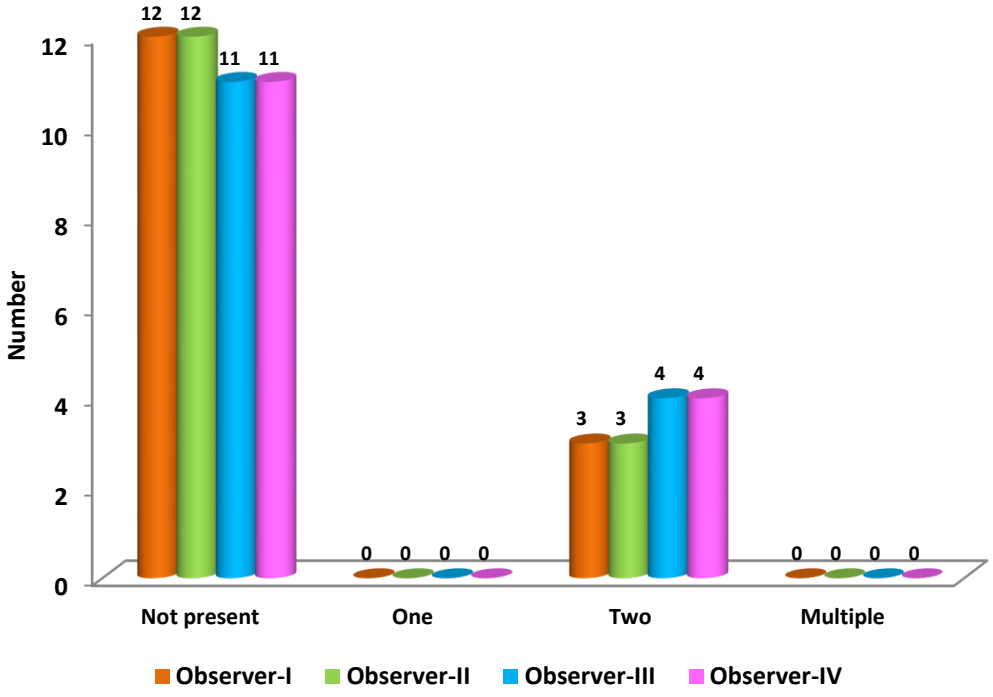

Graph-12: Comparison of strictures location between four observers

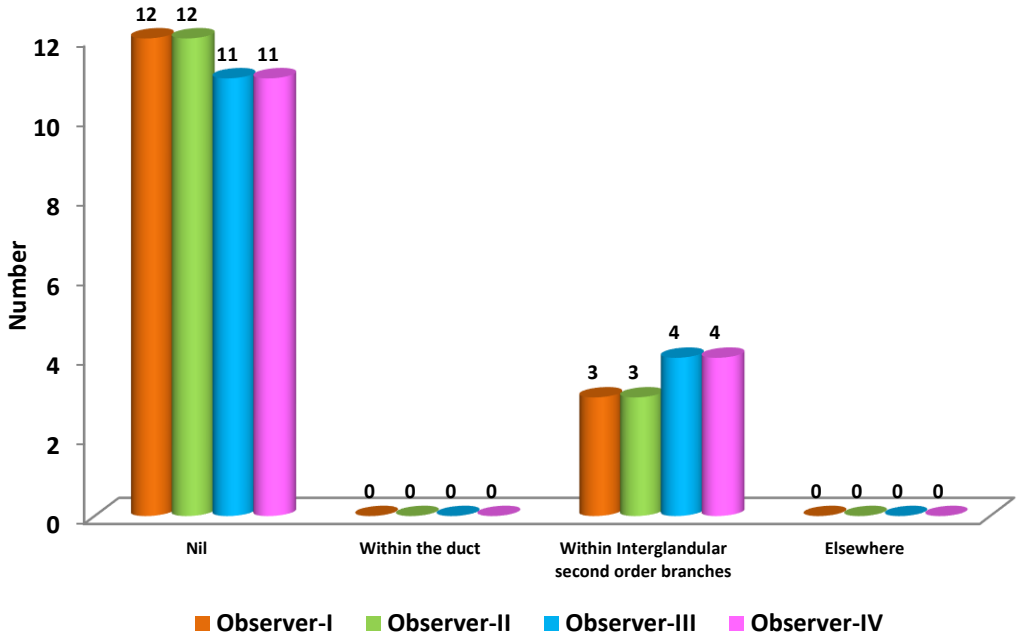

Graph-13: Comparison of strictures occludance between four observers

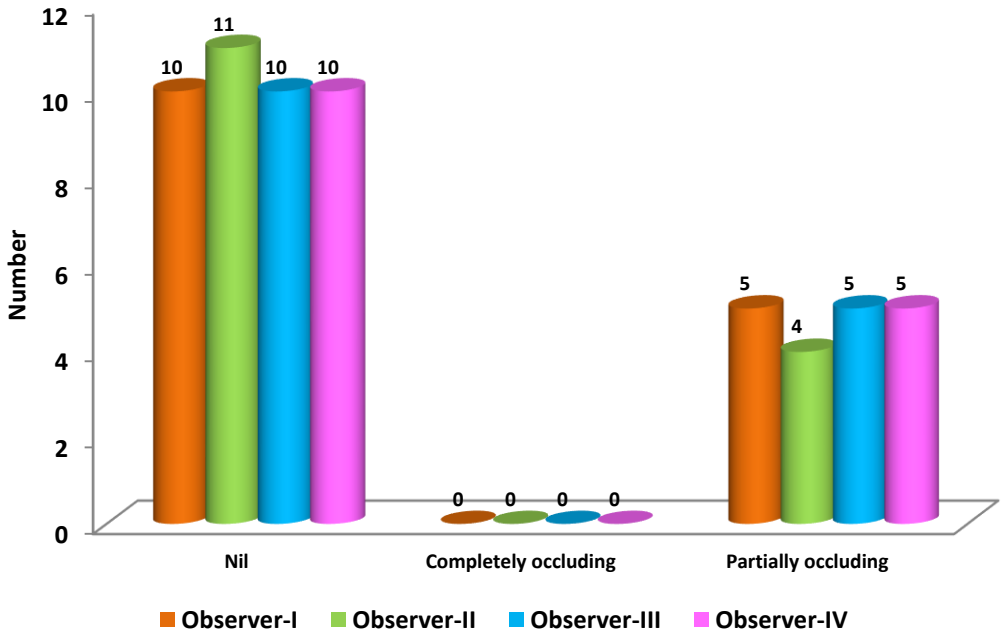

Graph-14: Comparison of ductal dilatation cause between four observers

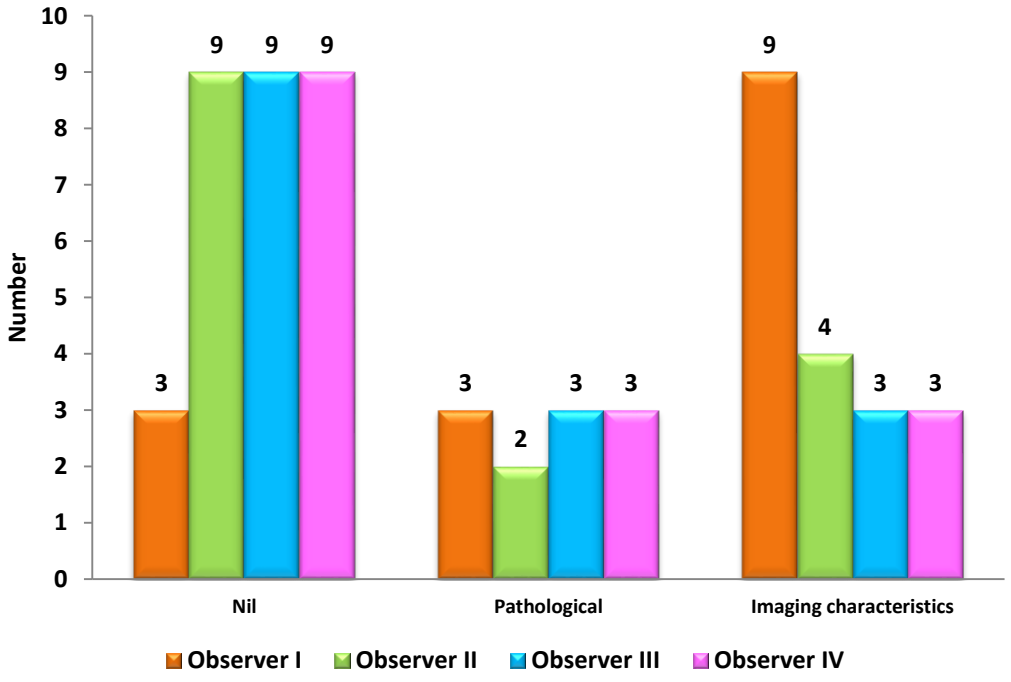

Graph-15: Comparison of ductal dilation severity between four observers

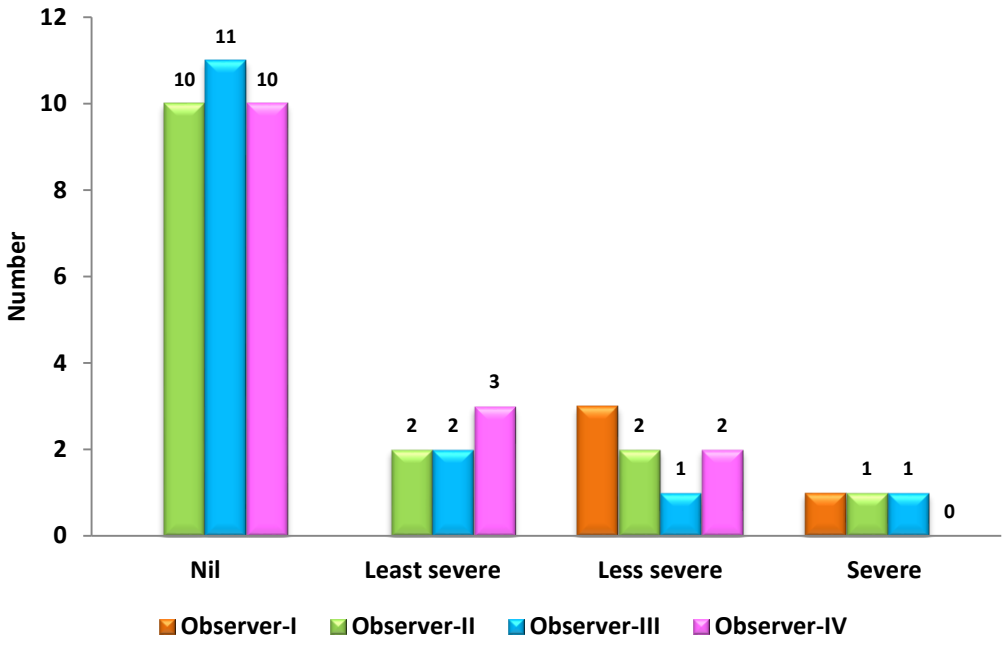

Graph-16: Comparison of acinar pooling number between four observers

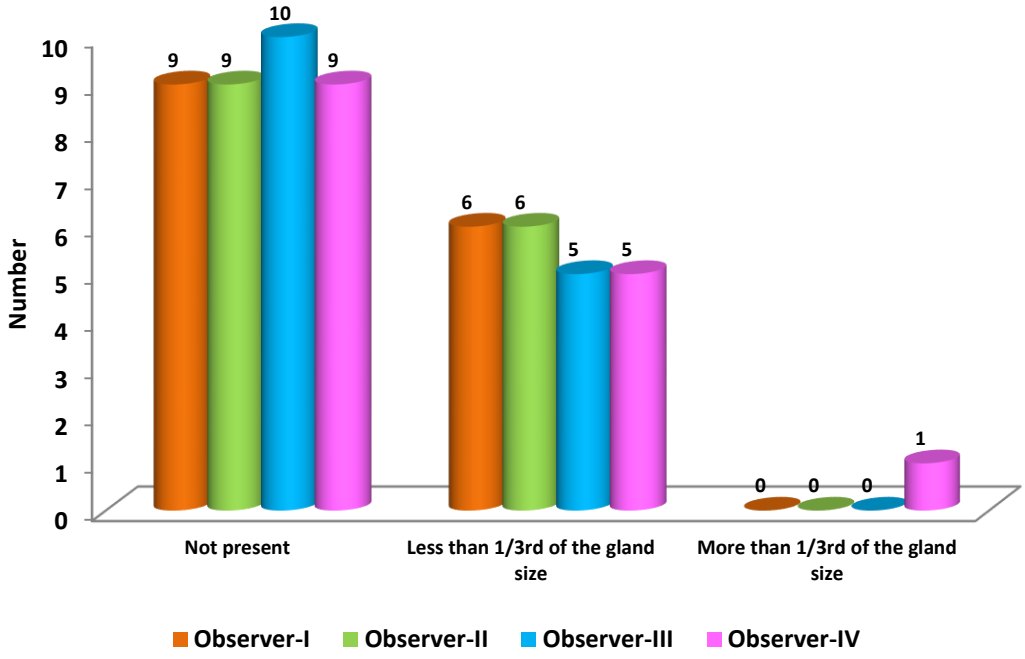

Graph-17: Comparison of mass number between four observers

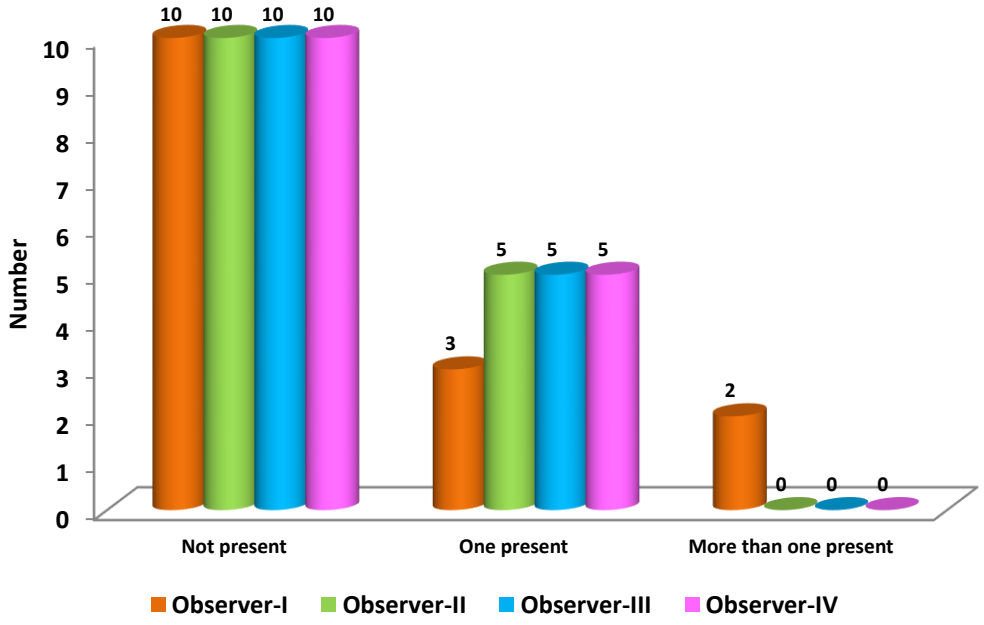

Graph-18: Comparison of mass borders between four observers

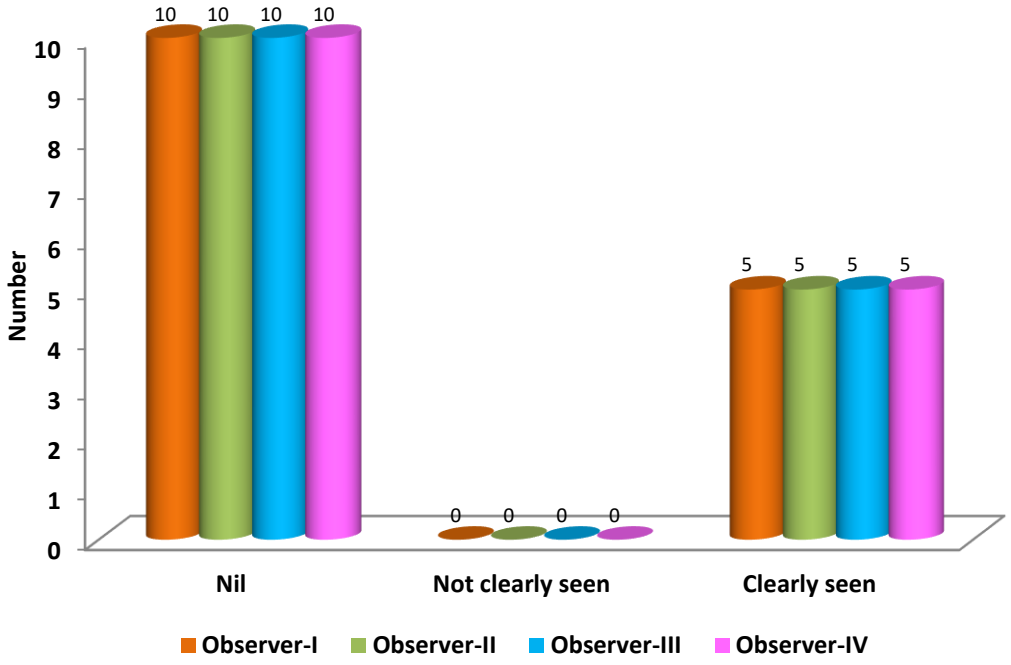

Graph-19: Comparison of mass internal structures between four observers

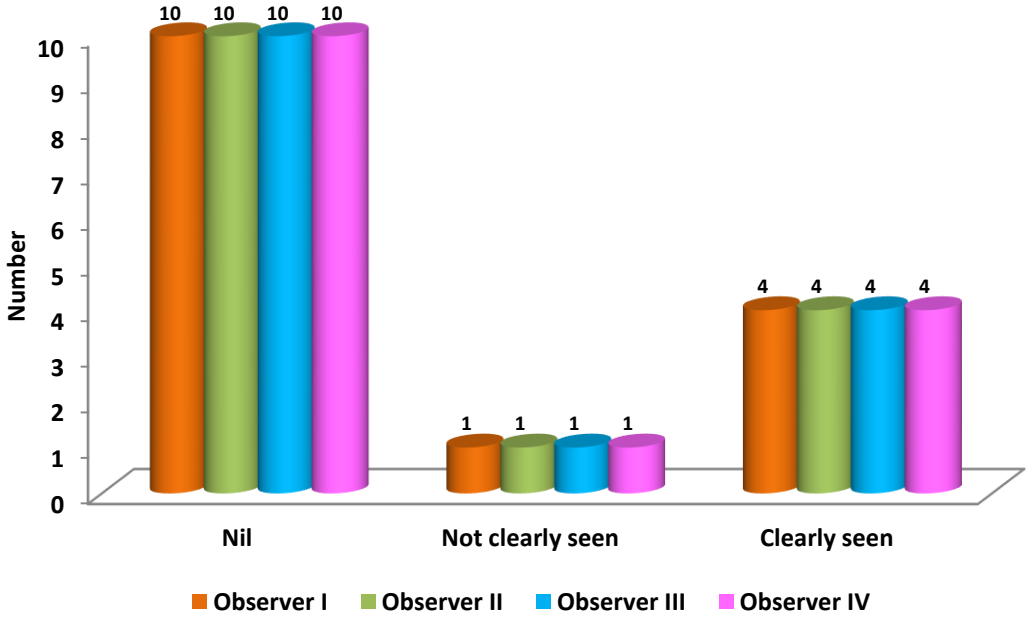

Graph-20: Comparison of mass effect on surrounding structures between four observers

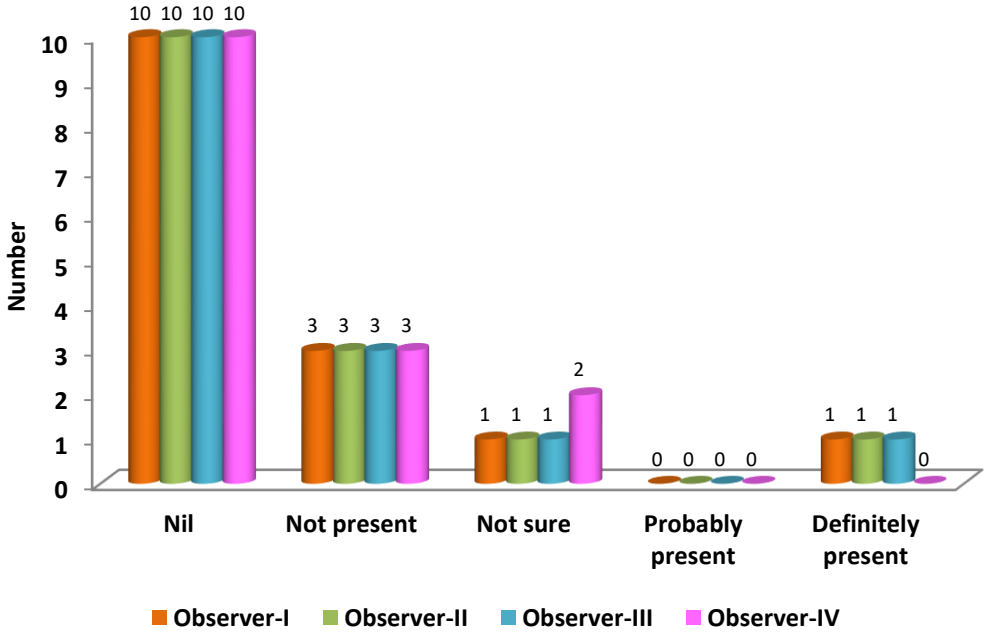

DISCUSSION

DISCUSSION

Sialography is the radiographic technique which has been used for years for the demonstration of major salivary gland pathologies by introduction of a contrast medium into their ductal system. It is useful for studying the ductal architecture along with the detection of salivary gland pathosis such as the presence of sialolith, strictures, ductal dilatation etc. Sialography has also got its own therapeutic value as it occasionally helps in releasing the occluding mucous plugs; due to the ductal dilatation caused by the intraluminal pressure of the injected contrast medium.

Over the years, sialography has been paired with various other radiographic techniques such as conventional imaging, computed tomography (CT), fluoroscopy, and magnetic resonance imaging (MRI). Ultrasonography is also used in major salivary gland imaging. Unfortunately, each of these radiographic modalities has got its own limitations, and these have affected the diagnostic accuracy of sialographic images. Conventional 2D images offers overlapping ductal architecture, which will reduce the accuracy of image interpretation. Fluoroscopy, being a real time imaging modality, it also suffers from overlapping anatomical structures. CT sialography and MRI sialography offers the advantage of multiplanar formatted view of the major salivary gland in all three planes, circumventing the problem of overlapping anatomical structures, even though its less spatial resolution limits their accuracy in the detection small sialoliths, strictures, and delicate ductal anatomy. Cost, accessibility, and longer imaging times are the other limitations of MDCT and MRI sialography.

Cone beam computed tomography is the imaging modality used predominantly in the field of maxillofacial diagnostics due to its high resolution isotropic images, low radiation dose and fast scanning time.[9,24] CBCT sialography allows 3D reconstruction along with the visualization of the ductal architecture in all possible dimensions. Combining the versatility of the CBCT with the benefits of the sialography would complement each other in the detection of salivary gland pathologies.

Several authors have classified major salivary gland diseases into neoplastic lesions, obstructive or inflammatory lesions and other systemic diseases.[6] Salivary gland neoplasms represent clinically as large masses associated with dull gnawing pain. In cases of salivary gland malignances, infiltration of the lesion to the overlying skin, cervical (regional) lymphadenopathy or facial nerve palsy may develop. Primary malignancies of salivary glands usually spread by regional lymphatics. There is a rule in salivary gland tumors, which states that smaller the size of the salivary gland, the higher is the rate of malignancy.[26] In contrast to salivary gland tumors, the obstructive and inflammatory conditions of major salivary glands manifest clinically with cardinal signs of inflammation such as pain and diffuse swelling of the gland. Obstruction of the major salivary gland may develop as a result of salivary calculi, ductal strictures, or even both. In such cases, radiographic imaging plays a pivotal role in the detection of the cause, extent, and effects of the obstruction within the major salivary glands.[3,4]

In this study, the normal ductal structure such as primary duct, secondary duct and parenchyma along with abnormal salivary gland pathologies such as the presence of sialolith, strictures, ductal dilatation, acinar pooling and space

occupying lesions were used as the criteria for the interpretation of CBCT sialography images. The study proved the accuracy of CBCT sialography in the evaluation of ductal architecture with associated pathologies, except that of ductal dilatation.

Literature only reports few studies regarding cone beam computed tomography sialography. CBCT sialography was first described by Drage NA and Brown JE in the year 2009, in a case report of two female patients with salivary gland obstruction.[47] Authors appreciated the easy visualization of ductal architecture along with salivary gland pathology which was consistent with our study. Unfortunately, they could not comment on the efficacy of CBCT sialography in the evaluation of space occupying lesions.

Varoquaux et al in 2011 studied the efficacy of sialography paired with cone beam computed tomography in assessing the salivary gland obstructions.[48]They concluded that CBCT sialography even helped in the demonstration of delicate parenchyma. Our study has also proved the same by interobserver concordance between the observers.

Jadu et al in 2013 conducted a series of researches with cone beam computed tomography sialography in the imaging of parotid and submandibular salivary glands.[1]They admitted the superiority of CBCT sialography in the demonstration of ductal architecture and in the evaluation of salivary gland pathologies. CBCT sialography also helped in the accurate image interpretation. This is attributed to the high resolution isotropic images produced by the CBCT machine without any overlapping of the anatomic structures. Based upon their study, CBCT sialography

proved to be an effective diagnostic tool in the detection of salivary gland pathologies. The results obtained by this study are consistent with our results.

Followed by Jadu et al, Nagla Abdel-Wahed et al in the year 2013 studied the primitive role of cone beam computed sialography over that of conventional sialography in diagnosis of major salivary gland lesions.[26] This study also confirmed the superiority of CBCT sialography over conventional sialography in demonstrating ductal pattern along with salivary gland abnormalities. The authors stated that CBCT sialography would help in better demonstration of the ductal architecture and can be used as a valuable diagnostic tool in the detection of salivary gland lesions. The final data obtained from this study is also found to be in concordance with that of our study.

In our study, the normal ductal architecture such as primary duct, secondary duct and parenchyma are better visualized in cone beam computed tomography in all multiplanar views, such as coronal, sagittal, axial and tangential views. The ductal outline is appreciated well in 3D rendered imaging format. Abnormal salivary gland findings such as sialolith, strictures, ductal dilatation, acinar pooling and space occupying lesions are also clearly visualized in all four planes. Strictures are detected by tracking the salivary gland in both coronal and sagittal views. Ductal dilatation are demonstrated by manipulating the cone beam computed tomography sialography images in sagittal view, axial view and also in 3D rendered imaging. Acinar pooling and space occupying lesions such as neoplasms are visualized and appreciated well in all multiplanar views along with 3D formatted image. CBCT sialography archival images in our study had series of cases which included Sjogren's syndrome, salivary gland neoplasms, and obstructive salivary gland

disorders such as strictures in the ductal architecture. A rare case with dual submandibular salivary gland on right side is also documented in our study. The results obtained showed high level of interobserver concordance, depicting the sensitivity of CBCT sialography. The shortcomings of conventional sialographic imaging techniques such as overlapping of ductal architecture are ruled out because of the ability of cone beam computed tomography to provide slice vise data of the area of interest to be visualized. Other limitations such as inappropriate detection of the effects of salivary gland neoplasms on adjacent structures and non-reliable measurement of salivary gland tumors are also ruled out due to the fact that CBCT provides isotropic images with high resolution.

The lacunae in all these researches are the standardized algorithm for interpretation of CBCT images, which has been put forth in our study. This will ensure in better understanding of CBCT images and will lead to proper diagnosis of the condition. Moreover, the high correlation of data between the four observers in interpreting the normal ductal structure such as primary duct, secondary duct and parenchyma along with abnormal salivary gland pathologies such as the presence of sialolith, strictures, acinar pooling and space occupying lesions shows the superiority and accuracy of CBCT sialography. Negative correlation between the observers was noted in terms of ductal dilatation because of the fact of interobserver variability between them, but increased sample size in cases with ductal dilatation would help in reevaluating the non-significance achieved. Finally, this study, with fifteen archival cone beam computed tomography sialography images confirmed the accuracy and superiority of CBCT sialography in the evaluation and detection of major salivary gland pathologies.

CONCLUSION

CONCLUSION

Diagnostic imaging plays a key role in the overall management of the disease condition and hence by leading to a proper way for the betterment of the patient's health. The role of diagnostic imaging as of now, with the advent of various new imaging modalities is no longer limited to provide an appropriate interpretation which will contribute to the diagnosis. CBCT is one such imaging modality, which totes the entire head and maxillofacial region, providing a better and clear descriptive view of each anatomic structures, in which CBCT sialography, is an interesting field which leads path to open up lot of exciting possibilities at the glandular acinar level, years ahead. It is a novel radio diagnostic technique for evaluating the ductal and glandular anatomy along with the detection of various pathosis of major salivary glands by combining the versatility of cone beam computed tomography with the benefits of sialography.

We have successfully put forth an algorithm through which the CBCT sialography images can be evaluated and proper diagnosis can be elicited. Future researches should be done with an increased sample size in order to incorporate more data regarding the same. In conclusion, CBCT sialography serves as a better diagnostic technique in case of major salivary gland imaging in patients suffering from salivary gland pathosis. Along with the proposed algorithm, the interpretation of CBCT sialography images can be done easily and accurately, ultimately leading to proper diagnosis, treatment plan and management of the major salivary gland disorders.

BIBLIOGRAPHY

BIBLIOGRAPHY

1. Jadu FM, Lam EW. A comparative study of the diagnostic capabilities of 2D plain radiograph and 3D cone beam CT sialography. Dentomaxillofacial Radiology 2013; 42(1):20110319.
2. Jäger L, Menauer F, Holzknecht N, Scholz V, Grevers G, Reiser M. Sialolithiasis: MR sialography of the submandibular duct - An alternative to conventional sialography and US?. Radiology 2000; 216(3):665-71.
3. Burke CJ, Thomas RH, Howlett D. Imaging the major salivary glands. British Journal of Oral and Maxillofacial Surgery 2011; 49(4):261-9.
4. Levy DM, ReMine WH, Devine KD. Salivary gland calculi: pain, swelling associated with eating. Jama 1962; 181(13):1115-9.
5. Benson BW. Salivary gland radiology. In: White SC, Pharoah MJ (eds). Oral radiology: principles and interpretation. 6th ed. St.Louis, MO: Mosby 2009; 11:578–98.
6. Yousem DM, Kraut MA, Chalian AA. Major salivary gland imaging. Radiology 2000; 216(1):19-29.
7. Rinast E, Gmelin E, Hollands-Thorn B. Digital subtraction sialography, conventional sialography, high-resolution ultrasonography and computed tomography in the diagnosis of salivary gland diseases. European journal of radiology 1989; 9(4):224-30.
8. Becker M, Marchal F, Becker CD, Dulguerov P, Georgakopoulos G, Lehmann W, Terrier F. Sialolithiasis and salivary ductal stenosis: diagnostic accuracy of MR sialography with a three-dimensional extended-phase conjugate-symmetry rapid spin-echo sequence. Radiology 2000; 217(2):347-58.

9. Miracle AC, Mukherji SK. Conebeam CT of the head and neck, part 2: clinical applications. American journal of neuroradiology 2009; 30(7):1285-92.
10. Yajima A, Otonari-Yamamoto M, Sano T, Hayakawa Y, Otonari T, Tanabe K, Wakoh M, Mizuta S, Yonezu H, Nakagawa K, Yajima Y. Cone-beam CT (CB Throne®) Applied to Dentomaxillofacial Region. The Bulletin of Tokyo Dental College 2006; 47(3):133-41.
11. Holmberg KV, Hoffman MP. Anatomy, biogenesis and regeneration of salivary glands. In Saliva: Secretion and Functions 2014 (Vol. 24, pp. 1-13). Karger Publishers.
12. Dale AC. Salivary Glands. In: Ten Cate AR (ed). Oral Histology: development, structure, and function. St. Louis, MO: Mosby, 1998; 356-88.
13. Som PC, Gensler MS. Anatomy and Pathology of the Salivary Glands. In: Som PC, Curtin HD. Head and Neck Imaging. St. Louis, MO: Elsevier, 2011.
14. Liebgott B. Applied Anatomy. The anatomical basis of dentistry 2nd Ed. St. Louis: Mosby, Inc. 2001:517-20.
15. Borysenko M, Beringer T. Oral Cavity and Alimentary Tract. In: Borysenko M, Beringer T. Functional Histology. Boston, MA: Little, Brown and Co 1984; 309-39.
16. Atkinson JC, Grisius M, Massey W. Salivary hypofunction and xerostomia: diagnosis and treatment. Dental Clinics 2005; 49(2):309-26.
17. La'Porte SJ, Juttla JK, Lingam RK. Imaging the floor of the mouth and the sublingual space. Radiographics 2011; 31(5):1215-30.
18. Liyanage SH, Spencer SP, Hogarth KM, Makdissi J. Imaging of salivary glands. Imaging 2007; 19(1):14-27.

19. Rastogi R, Bhargava S, Mallarajapatna GJ, Singh SK. Pictorial essay: Salivary gland imaging. The Indian journal of radiology & imaging 2012; 22(4):325.
20. Dhameja M, Singla V, Dhameja K, Singla N. Diagnostic Imaging of the Salivary Glands-A Review. International Journal of Contemporary Medicine Surgery and Radiology. 2016; 1(1):12-15.
21. Cho HW, Kim J, Choi J, Choi HS, Kim ES, Kim SH, Choi EC. Sonographically guided fine-needle aspiration biopsy of major salivary gland masses: a review of 245 cases. American Journal of Roentgenology 2011; 196(5):1160-3.
22. El-Khateeb SM, Abou-Khalaf AE, Farid MM, MA. A prospective study of three diagnostic sonographic methods in differentiation between benign and malignant salivary gland tumours. Dentomaxillofacial Radiology 2011; 40(8):476-85.
23. Bialek EJ, Jakubowski W, Zajkowski P, Szopinski KT, Osmolski A. US of the major salivary glands: anatomy and spatial relationships, pathologic conditions, and pitfalls. Radiographics 2006; 26(3):745-63.
24. Scarfe WC, Farman AG, Sukovic P. Clinical applications of cone-beam computed tomography in dental practice. Journal-Canadian Dental Association 2006; 72(1):75.
25. Abdel-Wahed N, Amer ME, Abo-Taleb NS. Assessment of the role of cone beam computed sialography in diagnosing salivary gland lesions. Imaging science in dentistry 2013; 43(1):17-23.
26. Faye N, Tassart M, Périé S, Deux JF, Kadi N, Marsault C. Imaging of salivary lithiasis. Journal de radiologie 2006; 87(1):9-15.

27. Shah VN, Branstetter IV BF. Oncocytoma of the parotid gland: a potential false-positive finding on 18F-FDG PET. American Journal of Roentgenology 2007; 189(4):W212-4.
28. Yuasa K, Nakhyama E, Ban S, Kawazu T, Chikui T, Shimizu M, Kanda S. Submandibular gland duct endoscopy: Diagnostic value for salivary duct disorders in comparison to conventional radiography, sialography, and ultrasonography. Oral Surgery, Oral Medicine, Oral Pathology, Oral Radiology, and Endodontology 1997; 84(5):578-81.
29. Cook TJ, Pollack J. Sialography: Pathologic-radiologic correlation. Oral Surgery, Oral Medicine, Oral Pathology 1966; 21(5):559-73.
30. Kalinowski M, Heverhagen JT, Rehberg E, Klose KJ, Wagner HJ. Comparative study of MR sialography and digital subtraction sialography for benign salivary gland disorders. American journal of neuroradiology 2002; 23(9):1485-92.
31. Ericson S. The importance of sialography for the determination of the parotid flow: The normal variation in salivary output in relation to the size of the gland at stimulation with citric acid. Acta oto-laryngologica 1971; 72(1-6):437-44.
32. Yune HY, Klatte EC. Current status of sialography. American Journal of Roentgenology 1972; 115(2):420-8.
33. Rose SS. Sialography in diagnosis. Postgraduate medical journal 1950; 26(300):521.
34. Verhoeven JW. Choice of contrast medium in sialography. Oral surgery, oral medicine, oral pathology 1984; 57(3):323-37.

35. Daniels TE, Benn DK. Is sialography effective in diagnosing the salivary component of Sjögren's syndrome?. Advances in dental research 1996; 10(1):25-8.
36. Schortinghuis J, Pijpe J, Spijkervet FK, Vissink A. Retention of lipiodol after parotid gland sialography. International journal of oral and maxillofacial surgery 2009; 38(4):346-9.
37. Reddy SS, Rakesh N, Raghav N, Devaraju D, Bijjal SG. Sialography: Report of 3 cases. Indian Journal of Dental Research 2009; 20(4):499.
38. Zhu W, Hu F, Liu X, Guo S, Tao Q. Role of the accessory parotid gland in the Etiology of Parotitis: statistical analysis of Sialographic features. PloS one 2016; 11(2):e0150212.
39. Wu CB, Zhou Q. To explore the role of sialography in the diagnosis of chronic parotitis. International Journal of Oral and Maxillofacial Surgery 2017; 46:375.
40. Tucci FM, Roma R, Bianchi A, De Vincentiis GC, Bianchi PM. Juvenile recurrent parotitis: diagnostic and therapeutic effectiveness of sialography. Retrospective study on 110 children. International journal of pediatric otorhinolaryngology 2019.
41. Hansson LG, Johansen CC. CT sialography and conventional sialography in the investigation of parotid masses. Oral surgery, oral medicine, oral pathology 1987; 64(4):494-500.
42. Jadu F, Yaffe MJ, Lam EW. A comparative study of the effective radiation doses from cone beam computed tomography and plain radiography for sialography. Dentomaxillofacial Radiology 2010; 39(5):257-63.

43. Shahidi S, Hamedani S. The feasibility of cone beam computed tomographic sialography in the diagnosis of space-occupying lesions: report of 3 cases. Oral surgery, oral medicine, oral pathology and oral radiology 2014; 117(6):e452-7.
44. Kroll T, May A, Wittekindt C, Kähling C, Sharma SJ, Howaldt HP, Klussmann JP, Streckbein P. Cone beam computed tomography (CBCT) sialography - an adjunct to salivary gland ultrasonography in the evaluation of recurrent salivary gland swelling. Oral surgery, oral medicine, oral pathology and oral radiology 2015; 120(6):771-5.
45. Chellathurai A, Gnanasigamani S, Kumaresan S, Balasubramaniam S, Damodarasamy K, Subbiah K, Kannappan S, Selvaraj B. Mr Sialography and conventional sialography in salivary gland and duct pathologies: a comparative study. Journal of evolution of medical and dental sciences 2016; 5(52):3467-72.
46. Bertin H, Bonnet R, Delemazure AS, Mourrain-Langlois E, Mercier J, Corre P. Three-dimensional cone-beam CT sialography in non tumour salivary pathologies: procedure and results. Dentomaxillofacial Radiology 2017; 46(1):20150431.
47. Drage NA, Brown JE. Cone beam computed sialography of sialoliths. Dentomaxillofacial Radiology 2009; 38(5):301-5.
48. Varoquaux A, Larribe M, Chossegros C, Cassagneau P, Salles F, Moulin G. Cone beam 3D sialography: preliminary study. Revue de stomatologie et de chirurgie maxillo-faciale 2011; 112(5):293-9.

ANNEXURE

SREE MOOKAMBIKA INSTITUTE OF DENTAL SCIENCES

KULASEKHARAM, KANYAKUMARI DIST., TAMIL NADU, INDIA.

INSTITUTIONAL RESEARCH COMMITTEE

Certificate

This is to certify that the research project protocol, ***Ref no. 13/08/2018*** titled, ***"Evaluation of Cone Beam Computed Tomography Sialography in diagnosing salivary gland lesions"*** submitted by ***Dr. Godwi Femine C.P., II Year MDS, Department of Oral Medicine & Radiology*** has been approved by the Institutional Research Committee at its meeting held on **18th *September 2018.***

Convener
Dr. T. Sreelal

Secretary
Dr. Vineet R.V

INSTITUTIONAL HUMAN ETHICS COMMITTEE

SREE MOOKAMBIKA INSTITUTE OF MEDICAL SCIENCES,
KULASEKHARAM, TAMILNADU

Communication of Decision of the Institutional Human Ethics Committee(IHEC)

SMIMS/IHEC No: 1 / Protocol no:48 / 2018

Protocol title:EVALUATION OF CONE BEAM COMPUTED TOMOGRAPHY SIALOGRAPHY IN DIAGNOSING SALIVARY GLAND LESIONS
Principal Investigator:Dr.Godwi Femine.C.P
Name& Address of Institution: Department of Oral Medicine & Radiology Sree Mookambika Institute of Dental Sciences ☑ New review ☐ Revised review ☐ Expedited review
Date of review (D/M/Y): 07-12-2018 Date of previous review , if revised application:
Decision of the IHEC: ☑ Recommended ☐ Recommended with suggestions ☐ Revision ☐ Rejected
Suggestions/ Reasons/ Remarks:
Recommended for a period of :One Year

Please note*

- Inform IHEC immediately in case of any Adverse events and Serious adverse events.
- Inform IHEC in case of any change of study procedure, site and investigator
- This permission is only for period mentioned above.
- Annual report to be submitted to IHEC.
- Members of IHEC have right to monitor the trial with prior intimation.

Reneega

Signature of Member Secretary (IHEC)

SREE MOOKAMBIKA INSTITUTE OF MEDICAL SCIENCES
IHEC
Date 19/12/18
KULASEKHARAM

DATA SHEET

Case no.	Question no.	Observer 1	Observer 2	Observer 3	Observer 4
1	1	2	2	2	2
	2	0	0	0	0
	3	2	2	2	2
	4	0	1	0	0
	5	2	2	2	2
	6	3	3	0	3
	7	0	0	0	0
	8	0	0	0	0
	9	0	0	0	0
	10	0	0	0	0
	11	0	0	0	0
	12	0	0	0	0
	13	0	0	0	0
	14	0	0	0	0
	15	0	0	0	0
	16	0	0	0	0
	17	2	1	1	1
	18	2	2	2	2
	19	2	2	2	2
	20	1	1	1	1
2	1	2	2	2	2
	2	0	0	0	0
	3	2	2	2	2
	4	0	1	0	0
	5	2	2	2	2
	6	0	3	0	3
	7	0	0	0	0
	8	0	0	0	0
	9	0	0	0	0
	10	0	0	0	0
	11	0	0	0	0
	12	0	0	0	0
	13	0	0	0	0
	14	0	0	0	0
	15	0	0	0	0
	16	0	0	0	0
	17	2	1	1	1
	18	2	2	2	2
	19	2	2	2	2
	20	1	1	1	1

Case no.	Question no.	Observer 1	Observer 2	Observer 3	Observer 4
3	1	2	2	2	2
	2	0	0	0	0
	3	2	2	2	2
	4	0	0	0	0
	5	2	2	2	2
	6	3	3	3	3
	7	0	0	0	0
	8	0	0	0	0
	9	0	0	0	0
	10	0	0	0	0
	11	0	0	3	3
	12	0	0	2	2
	13	0	0	2	2
	14	2	0	0	0
	15	1	0	0	0
	16	0	0	0	0
	17	1	1	1	1
	18	2	2	2	2
	19	1	1	1	1
	20	2	2	2	2
4	1	1	1	1	1
	2	1	1	1	1
	3	2	2	2	2
	4	0	0	0	0
	5	2	2	2	2
	6	0	0	0	0
	7	0	0	0	0
	8	0	0	0	0
	9	0	0	0	0
	10	0	0	0	0
	11	3	3	3	3
	12	2	2	2	2
	13	2	2	2	2
	14	2	0	0	0
	15	2	0	0	0
	16	1	1	1	1
	17	0	0	0	0
	18	0	0	0	0
	19	0	0	0	0
	20	0	0	0	0

Case no.	Question no.	Observer 1	Observer 2	Observer 3	Observer 4
5	1	2	2	2	2
	2	0	0	0	0
	3	2	2	2	2
	4	0	0	0	0
	5	2	2	2	2
	6	3	3	3	3
	7	0	0	0	0
	8	0	0	0	0
	9	0	0	0	0
	10	0	0	0	0
	11	0	0	0	0
	12	0	0	0	0
	13	2	2	2	2
	14	2	2	2	2
	15	0	0	0	0
	16	0	0	0	0
	17	1	1	1	1
	18	2	2	2	2
	19	2	2	2	2
	20	4	4	4	2
6	1	2	2	2	2
	2	0	0	0	0
	3	2	2	2	2
	4	0	0	0	0
	5	2	2	2	2
	6	3	3	3	3
	7	0	0	0	0
	8	0	0	0	0
	9	0	0	0	0
	10	0	0	0	0
	11	0	0	0	0
	12	0	0	0	0
	13	2	0	0	0
	14	1	0	0	0
	15	0	0	0	0
	16	0	0	0	0
	17	1	1	1	1
	18	2	2	2	2
	19	2	2	2	2
	20	1	1	1	1

Case no.	Question no.	Observer 1	Observer 2	Observer 3	Observer 4
7	1	2	2	2	2
	2	0	0	0	0
	3	2	2	2	2
	4	0	0	0	0
	5	2	2	2	2
	6	3	3	3	3
	7	0	0	0	0
	8	0	0	0	0
	9	0	0	0	0
	10	0	0	0	0
	11	3	3	3	3
	12	2	2	2	2
	13	2	2	2	2
	14	1	1	1	1
	15	2	2	2	2
	16	1	1	1	2
	17	0	0	0	0
	18	0	0	0	0
	19	0	0	0	0
	20	0	0	0	0
8	1	1	1	1	1
	2	0	0	0	0
	3	0	0	0	0
	4	1	1	1	1
	5	2	2	2	2
	6	3	3	3	3
	7	0	0	0	0
	8	0	0	0	0
	9	0	0	0	0
	10	0	0	0	0
	11	0	0	0	0
	12	0	0	0	0
	13	0	0	0	0
	14	2	0	0	0
	15	1	0	0	0
	16	1	1	1	1
	17	0	0	0	0
	18	0	0	0	0
	19	0	0	0	0
	20	0	0	0	0

Case no.	Question no.	Observer 1	Observer 2	Observer 3	Observer 4
9	1	2	2	2	2
	2	0	0	0	0
	3	2	2	2	2
	4	0	0	0	0
	5	2	2	2	2
	6	3	3	3	3
	7	0	0	0	0
	8	0	0	0	0
	9	0	0	0	0
	10	0	0	0	0
	11	0	0	0	0
	12	0	0	0	0
	13	0	0	0	0
	14	2	2	2	2
	15	1	1	0	1
	16	1	1	0	1
	17	0	0	0	0
	18	0	0	0	0
	19	0	0	0	0
	20	0	0	0	0
10	1	2	2	2	2
	2	0	0	0	0
	3	2	2	2	2
	4	0	0	0	0
	5	2	2	2	2
	6	3	3	3	3
	7	0	0	0	0
	8	0	0	0	0
	9	0	0	0	0
	10	0	0	0	0
	11	0	0	0	0
	12	0	0	0	0
	13	0	0	0	0
	14	2	2	1	1
	15	1	1	1	1
	16	1	1	1	1
	17	0	0	0	0
	18	0	0	0	0
	19	0	0	0	0
	20	0	0	0	0

Case no.	Question no.	Observer 1	Observer 2	Observer 3	Observer 4
11	1	2	2	2	2
	2	3	0	0	0
	3	2	2	2	2
	4	0	0	0	0
	5	1	2	2	2
	6	0	0	0	0
	7	2	0	0	0
	8	2	0	0	0
	9	1	0	0	0
	10	1	0	0	0
	11	0	0	0	0
	12	0	0	0	0
	13	0	0	0	0
	14	1	1	1	1
	15	3	3	3	2
	16	0	0	0	0
	17	0	0	0	0
	18	0	0	0	0
	19	0	0	0	0
	20	0	0	0	0
12	1	1	1	1	1
	2	1	1	1	1
	3	2	2	2	2
	4	0	0	0	0
	5	2	2	2	2
	6	0	0	0	0
	7	0	0	0	0
	8	0	0	0	0
	9	0	0	0	0
	10	0	0	0	0
	11	3	3	3	3
	12	2	2	2	2
	13	2	2	2	2
	14	2	2	2	2
	15	2	2	1	1
	16	1	1	1	1
	17	0	0	0	0
	18	0	0	0	0
	19	0	0	0	0
	20	0	0	0	0

Case no.	Question no.	Observer 1	Observer 2	Observer 3	Observer 4
13	1	2	2	2	2
	2	0	0	0	0
	3	2	2	2	2
	4	0	0	0	0
	5	2	2	2	2
	6	0	0	0	0
	7	0	0	0	0
	8	0	0	0	0
	9	0	0	0	0
	10	0	0	0	0
	11	0	0	0	0
	12	0	0	0	0
	13	0	0	0	0
	14	0	0	0	0
	15	0	0	0	0
	16	0	0	0	0
	17	0	0	0	0
	18	0	0	0	0
	19	0	0	0	0
	20	0	0	0	0
14	1	2	2	2	2
	2	0	0	0	0
	3	2	2	2	2
	4	0	0	0	0
	5	2	2	2	2
	6	0	0	0	0
	7	0	0	0	0
	8	0	0	0	0
	9	0	0	0	0
	10	0	0	0	0
	11	0	0	0	0
	12	0	0	0	0
	13	0	0	0	0
	14	2	0	0	0
	15	1	0	0	0
	16	0	0	0	0
	17	0	0	0	0
	18	0	0	0	0
	19	0	0	0	0
	20	0	0	0	0

Case no.	Question no.	Observer 1	Observer 2	Observer 3	Observer 4
15	1	2	2	2	2
	2	0	0	0	0
	3	2	2	2	2
	4	0	0	0	0
	5	2	2	2	2
	6	0	0	0	0
	7	0	0	0	0
	8	0	0	0	0
	9	0	0	0	0
	10	0	0	0	0
	11	0	0	0	0
	12	0	0	0	0
	13	0	0	0	0
	14	2	0	0	0
	15	1	0	0	0
	16	0	0	0	0
	17	0	0	0	0
	18	0	0	0	0
	19	0	0	0	0
	20	0	0	0	0